Electronic Supplementary Material (ESI) for RSC Sustainability.
This journal is © The Royal Society of Chemistry 2023

Sustainable approach for the synthesis of Chiral β-aminoketones using Encapsulated Chiral Zn(II)-Salen complex

Pratikkumar Lakhani[a], Sanjeev Kane[b], Himanshu Srivastava[b], U. K. Goutam[c], Chetan K. Modi*[,a]

[a]*Applied Chemistry Department, Faculty of Technology and Engineering, The Maharaja Sayajirao University of Baroda, Vadodara-390001*

[b]*Synchrotrons Utilisation Section, Raja Ramanna Centre for Advanced Technology, Indore 452013, India*

[c]*Technical Physics Division, Bhabha Atomic Research Centre, Mumbai-400085, India*

E-mail: chetanmodi-appchem@msubaroda.ac.in

Supporting Information

Table of Contents

1. Materials

SiO_2, HMI, zinc acetate, (-)-trans-1,2-diaminocyclohexane, salicylaldehyde and methanol (MeOH) was procured from Merck, India. The other chemicals used were aldehydes, ethyl acetoacetate, and urea, sourced from Loba Chemie, India. It is important to note that all of these reagents are of analytical grade and should be used without further purification once received.

2. Characterization Techniques

For the characterization of as-prepared materials such as neat MWW zeolite, Zn(II)-exchanged MWW zeolite and chiral Zn(II)-Salen@MWW catalyst different physicochemical techniques have been employed. XPS spectra were performed on Specs, Phoibios 225 spectrometer with Al Kα radiation (1486.6 eV), Synchrotrons Utilisation Section, Raja Ramanna Centre for Advanced Technology, Indore, India. The structure determinations of as-prepared materials were performed on Bruker AXS D8 Advance X-ray powder diffractometer with a CuKα (λ=1.54058) target and movable detector, which scans the intensity of diffracted radiation within the range of 5°–80° as a function of the angle 2θ between the incident and diffracted beams. Field Emission Scanning Electron Microscopes (FE-SEM), the images were taken at 5 keV and as-prepared materials was performed on Model FE-SEM: Auriga HT Make: Carl Zeiss Model at Synchrotrons Utilisation Section, Raja Ramanna Centre for Advanced Technology, Indore, India. The images were taken at 5 keV. BET surface area and pore size distribution measure on micromeritics. FTIR spectra of as prepared materials were performed in the range: 4000-400 cm^{-1} on a model: FTIR - 8400S Shimadzu using KBr pellets. EDX analysis on JSM-IT800 Schottky Field Emission Scanning Electron Microscope, JEOL at the Department of Metallurgical and Materials Engineering, Faculty of Technology & Engineering, The Maharaja Sayajirao University of Baroda, Vadodara, India.

3. Spectral Data for chiral Salen ligand

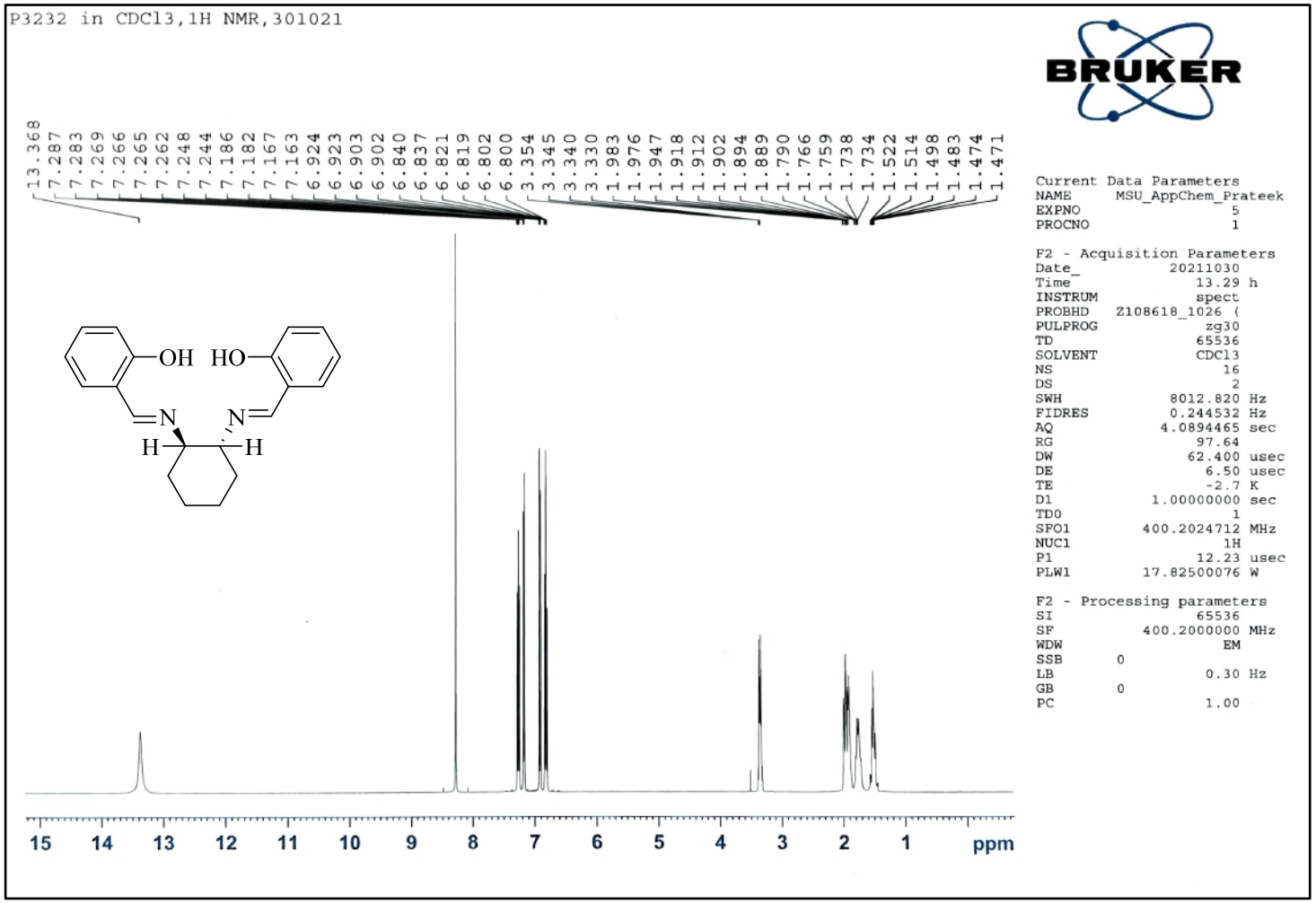

Fig. S1. ^{1}H NMR spectra of the chiral Salen ligand.

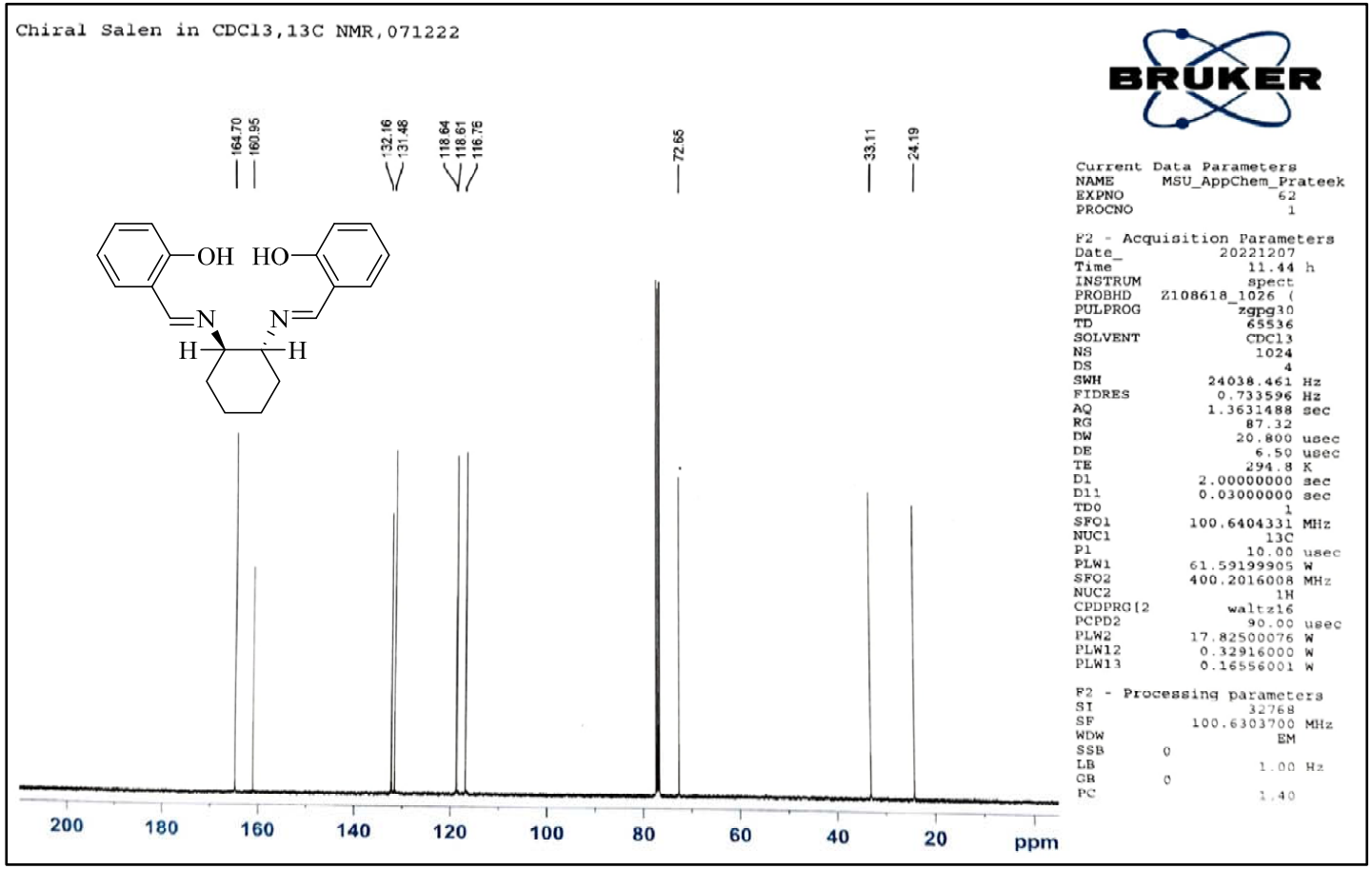

Fig. S2. ^{13}C NMR spectra of the Salen ligand.

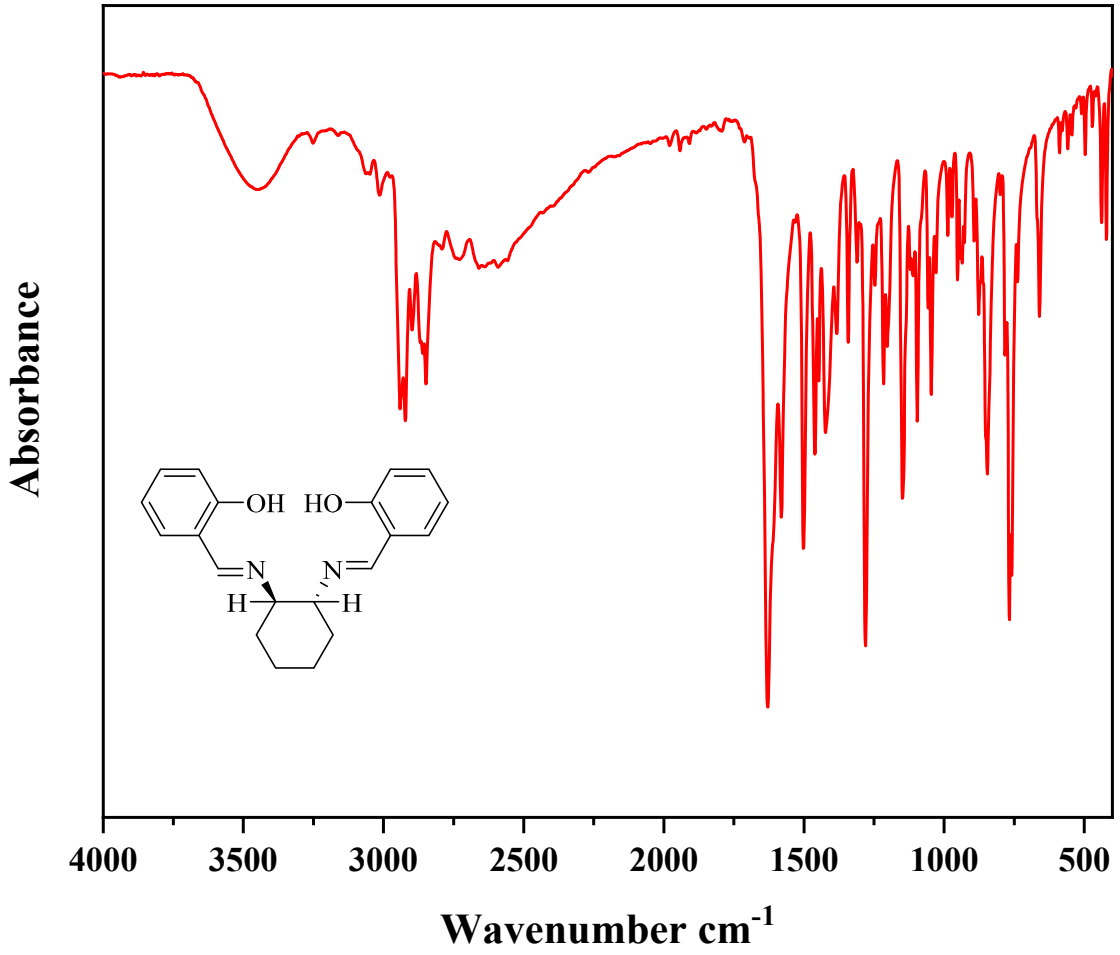

Fig. S3. FTIR spectra of the Salen ligand.

4. Characterization data for varying catalysts

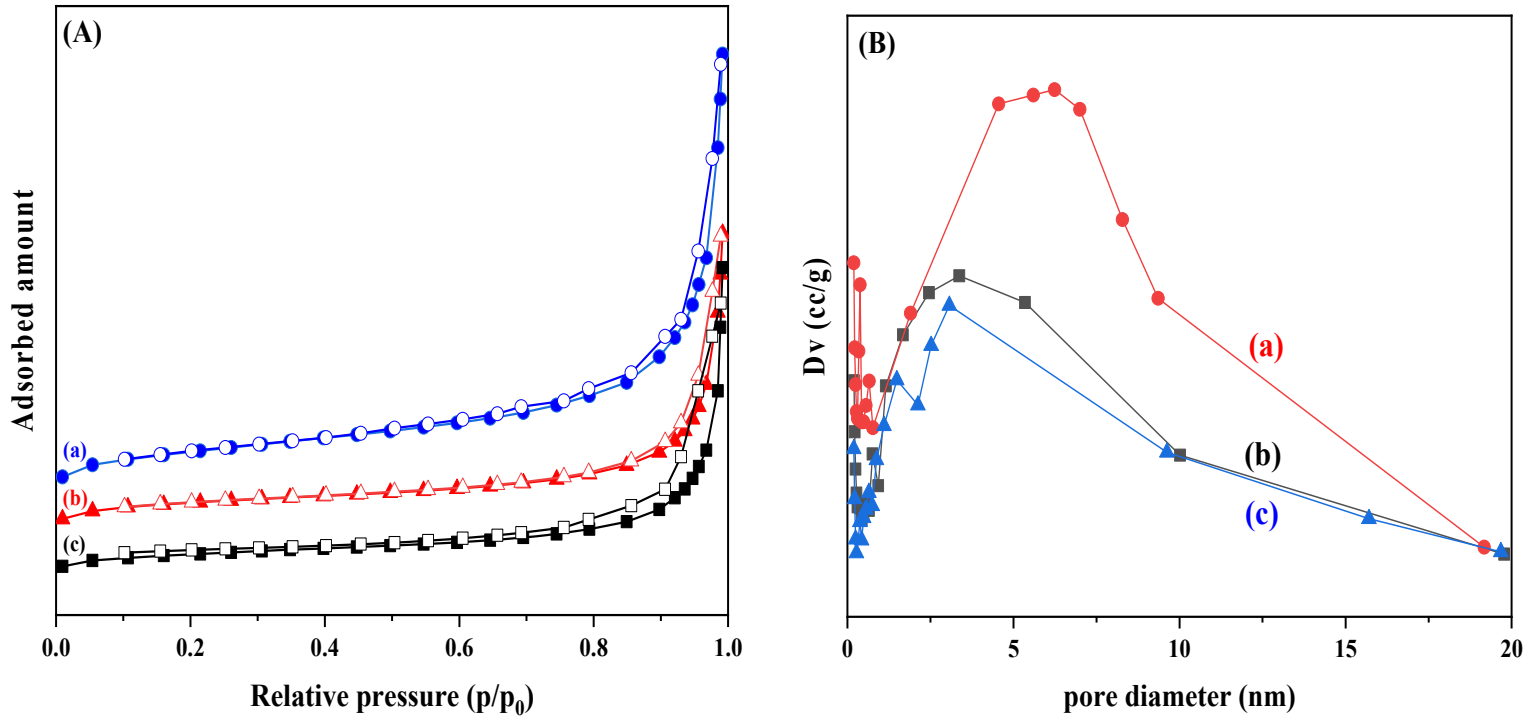

Fig. S4. (A) N_2 adsorption− desorption isotherms of (a) MWW zeolite (b) Zn(II)-exchanged MWW zeolite and (c) chiral Zn(II)-Salen@MWW catalyst; **(B)** BJH pore size distributions of (a) MWW zeolite (b) Zn(II)-exchanged MWW zeolite and (c) chiral Zn(II)-Salen@MWW catalyst.

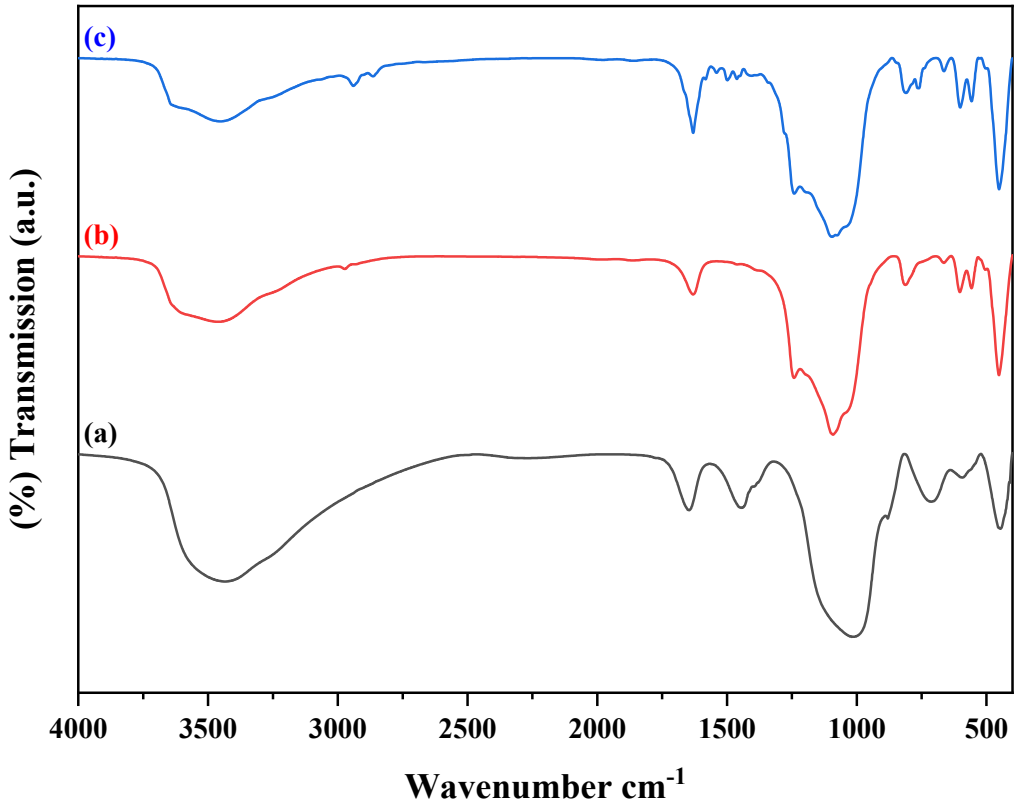

Fig. S5. FTIR spectra of (a) MWW zeolite (b) Zn(II)-exchanged MWW zeolite and (c) chiral Zn(II)-Salen@MWW catalyst.

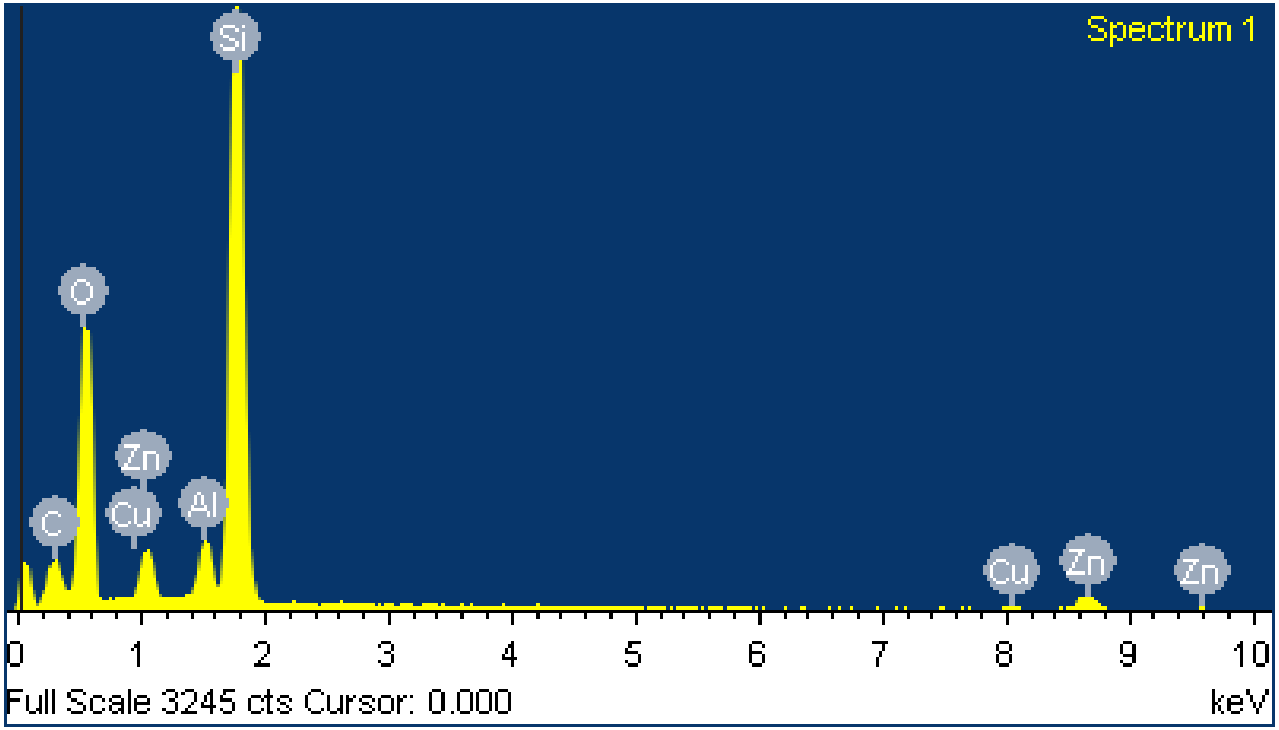

Fig. S6. EDX pattern of chiral Zn(II)-Salen@MWW catalyst

5. Chromatographic data for products

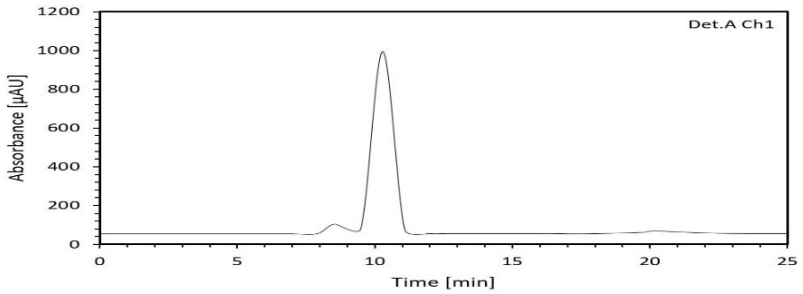

1st cycle of encapsulated chiral Zn(II) salen complex as a catalyst			
Peak	Ret. Time	Area	Area %
1	8.56	415753	02.71
2	10.29	14936723	97.29
Total		15352476	100

Fig. S7. Chiral HPLC spectra of the product (A).

Column: Chiralpak OJ-H (250 x 4.6) mm, 20µ (make: Diacel), Flow rate: 1.0 mL/min, Detection: 254 nm.

Enantiomeric excess (ee%) was calculated from the chromatographic data by the following equation:

$$(\text{ee}\%) = \left[\frac{peak\ area\ 1 - peak\ area\ 2}{peak\ area\ 1 + peak\ area\ 2}\right] \times 100$$

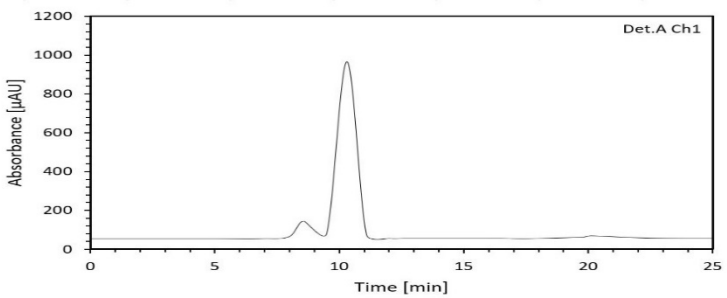

Fig. S8. Chiral HPLC spectra of the product (A2).

2nd cycle of encapsulated chiral Zn(II) salen complex as a catalyst			
Peak	Ret. Time	Area	Area %
1	8.58	417579	03.51
2	10.31	11481622	96.49
Total		11899201	100

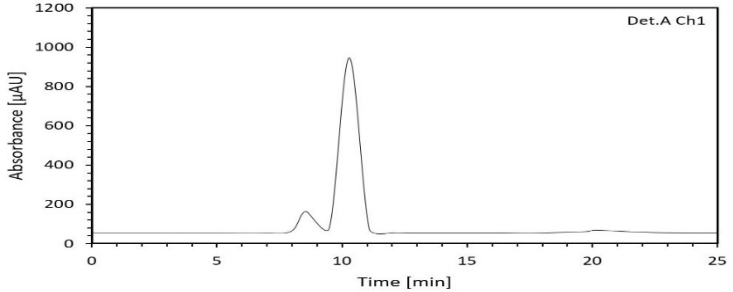

Fig. S9. Chiral HPLC spectra of the product (A3).

3rd cycle of encapsulated chiral Zn(II) salen complex as a catalyst			
Peak	Ret. Time	Area	Area %
1	8.57	651837	06.08
2	10.29	10063966	93.92
Total		10715803	100

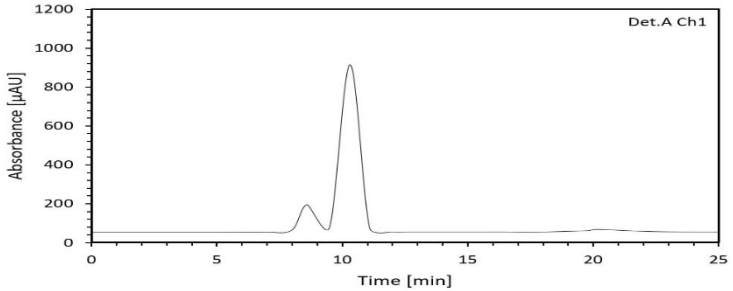

Fig. S10. Chiral HPLC spectra of the product (A4).

4th cycle of encapsulated chiral Zn(II) salen complex as a catalyst			
Peak	Ret. Time	Area	Area %
1	8.60	875743	08.04
2	10.31	10015123	91.96
Total		10890866	100

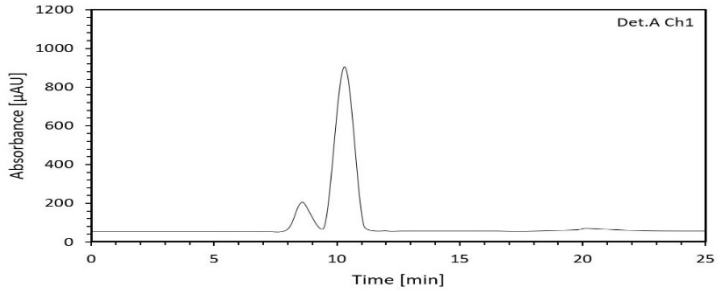

Fig. S11. Chiral HPLC spectra of the product (A5).

5th cycle of encapsulated chiral Zn(II) salen complex as a catalyst			
Peak	Ret. Time	Area	Area %
1	8.58	935124	08.78
2	10.30	9718459	91.22
Total		10653583	100

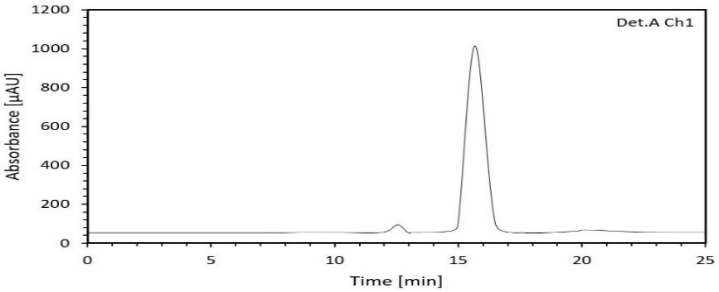

Fig. S12. Chiral HPLC spectra of the product (B).

4-NO_2 Benzaldehyde as a reactant			
Peak	Ret. Time	Area	Area %
1	12.55	331419	01.83
2	15.68	17763954	98.17
Total		18095373	100

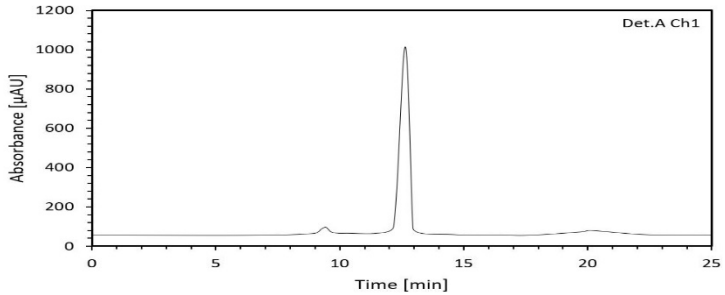

Fig. S13. Chiral HPLC spectra of the product (C).

4-Me Benzaldehyde as a reactant			
Peak	Ret. Time	Area	Area %
1	09.45	390125	02.30
2	12.65	16576347	97.70
Total		16966472	100

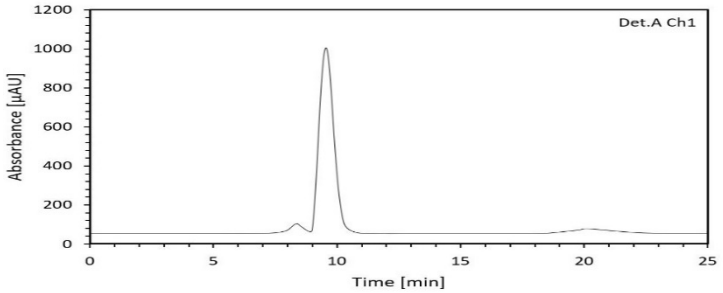

Fig. S14. Chiral HPLC spectra of the product (D).

4-OH Benzaldehyde as a reactant			
Peak	Ret. Time	Area	Area %
1	08.40	812219	05.13
2	09.56	15011239	94.87
Total		15823458	100

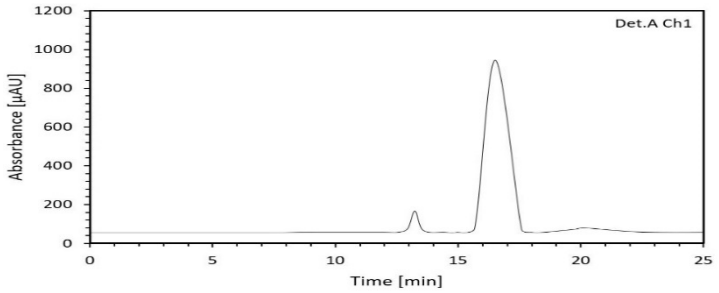

Fig. S15. Chiral HPLC spectra of the product (E).

4-Cl Benzaldehyde as a reactant			
Peak	Ret. Time	Area	Area %
1	13.25	803443	05.27
2	16.51	14441143	94.73
Total		15244586	100

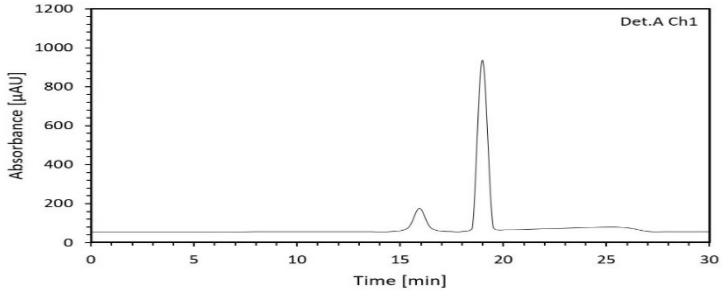

Fig. S16. Chiral HPLC spectra of the product (F).

4-OMe Benzaldehyde as a reactant			
Peak	Ret. Time	Area	Area %
1	15.93	648511	05.95
2	18.98	10249311	94.05
Total		10897822	100

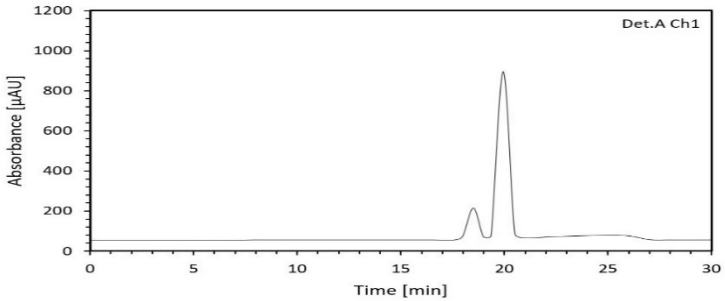

Fig. S17. Chiral HPLC spectra of the product (G).

2-OH Benzaldehyde as a reactant			
Peak	Ret. Time	Area	Area %
1	18.50	946287	07.96
2	19.93	10936284	92.04
Total		11882571	100

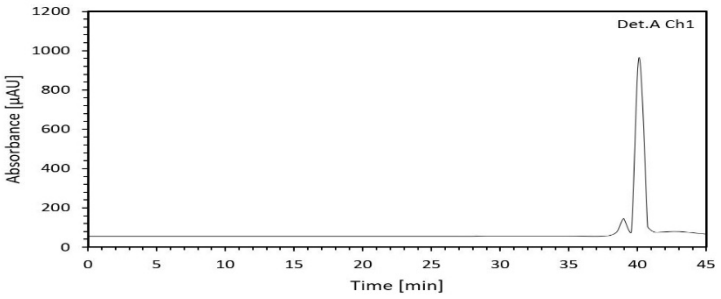

Fig. S18. Chiral HPLC spectra of the product (H).

4-OH Aniline as a reactant			
Peak	Ret. Time	Area	Area %
1	38.99	431298	04.09
2	40.10	10116190	95.91
Total		10547488	100

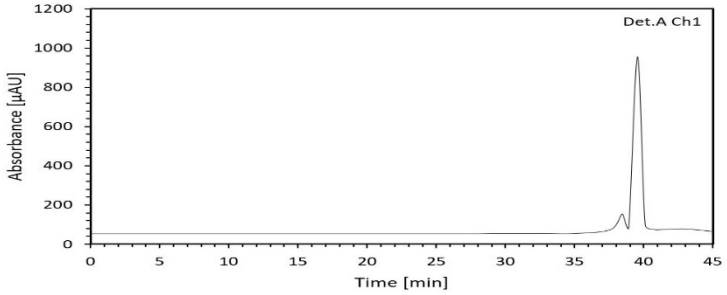

Fig. S19. Chiral HPLC spectra of the product (I).

4-OMe Aniline as a reactant			
Peak	Ret. Time	Area	Area %
1	38.45	794312	05.21
2	39.53	14452312	94.79
Total		15246624	100

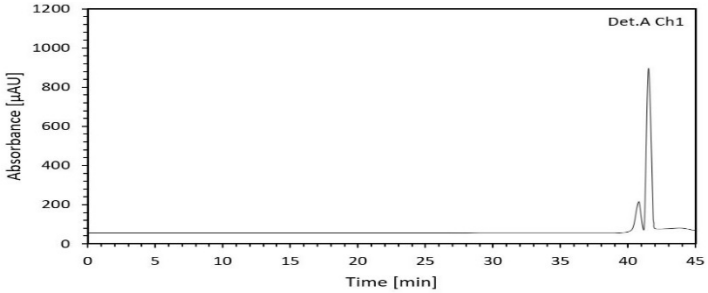

Fig. S20. Chiral HPLC spectra of the product (J).

2-OH Aniline as a reactant			
Peak	Ret. Time	Area	Area %
1	40.79	975743	08.14
2	41.50	11015123	91.86
Total		11990866	100

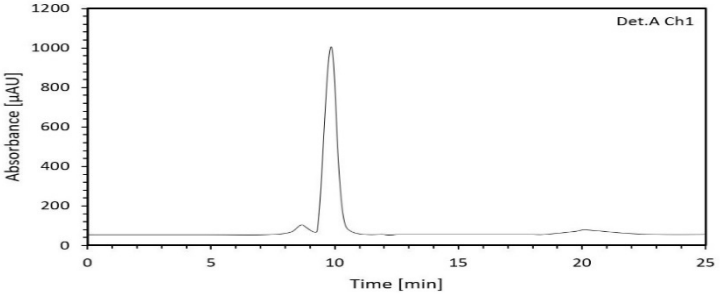

Fig. S21. Chiral HPLC spectra of the product (K).

Acetone as a reactant			
Peak	Ret. Time	Area	Area %
1	08.70	416367	02.82
2	09.86	14338791	97.18
Total		14755158	100

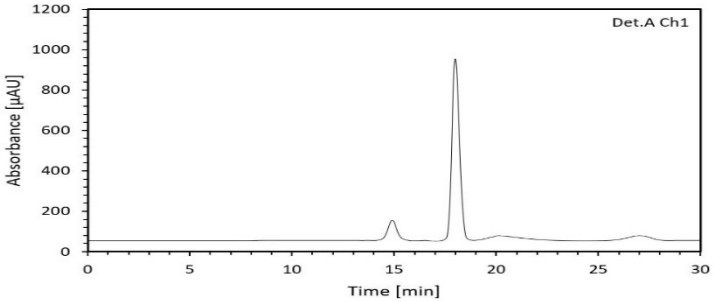

Fig. S22. Chiral HPLC spectra of the product (L).

4-Cl Acetophenone as a reactant			
Peak	Ret. Time	Area	Area %
1	14.90	836739	05.02
2	17.99	15827437	94.98
Total		16664176	100

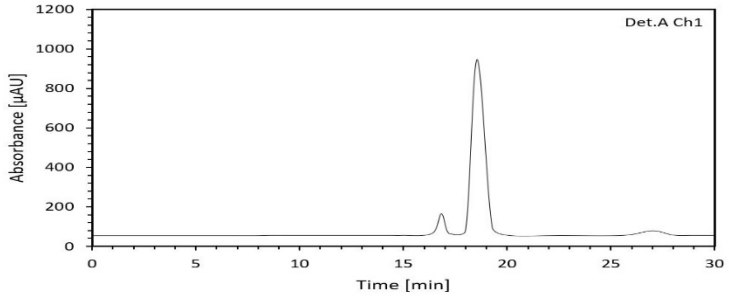

Fig. S23. Chiral HPLC spectra of the product (M).

4-Br Acetophenone as a reactant			
Peak	Ret. Time	Area	Area %
1	16.82	785401	05.52
2	18.55	13451416	94.48
Total		14236817	100

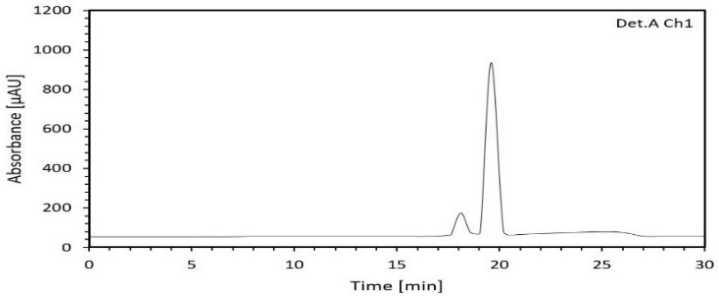

Fig. S24. Chiral HPLC spectra of the product (N).

4-OMe Acetophenone as a reactant			
Peak	Ret. Time	Area	Area %
1	18.12	679121	06.16
2	19.59	10342389	93.84
Total		11021510	100

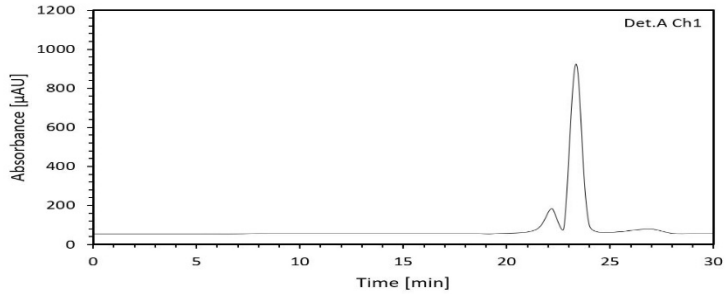

Fig. S25. Chiral HPLC spectra of the product (O).

4-OH Acetophenone as a reactant			
Peak	Ret. Time	Area	Area %
1	22.19	906736	06.51
2	23.35	13028246	93.49
Total		13934982	100

6. NMR and FTIR spectra for products

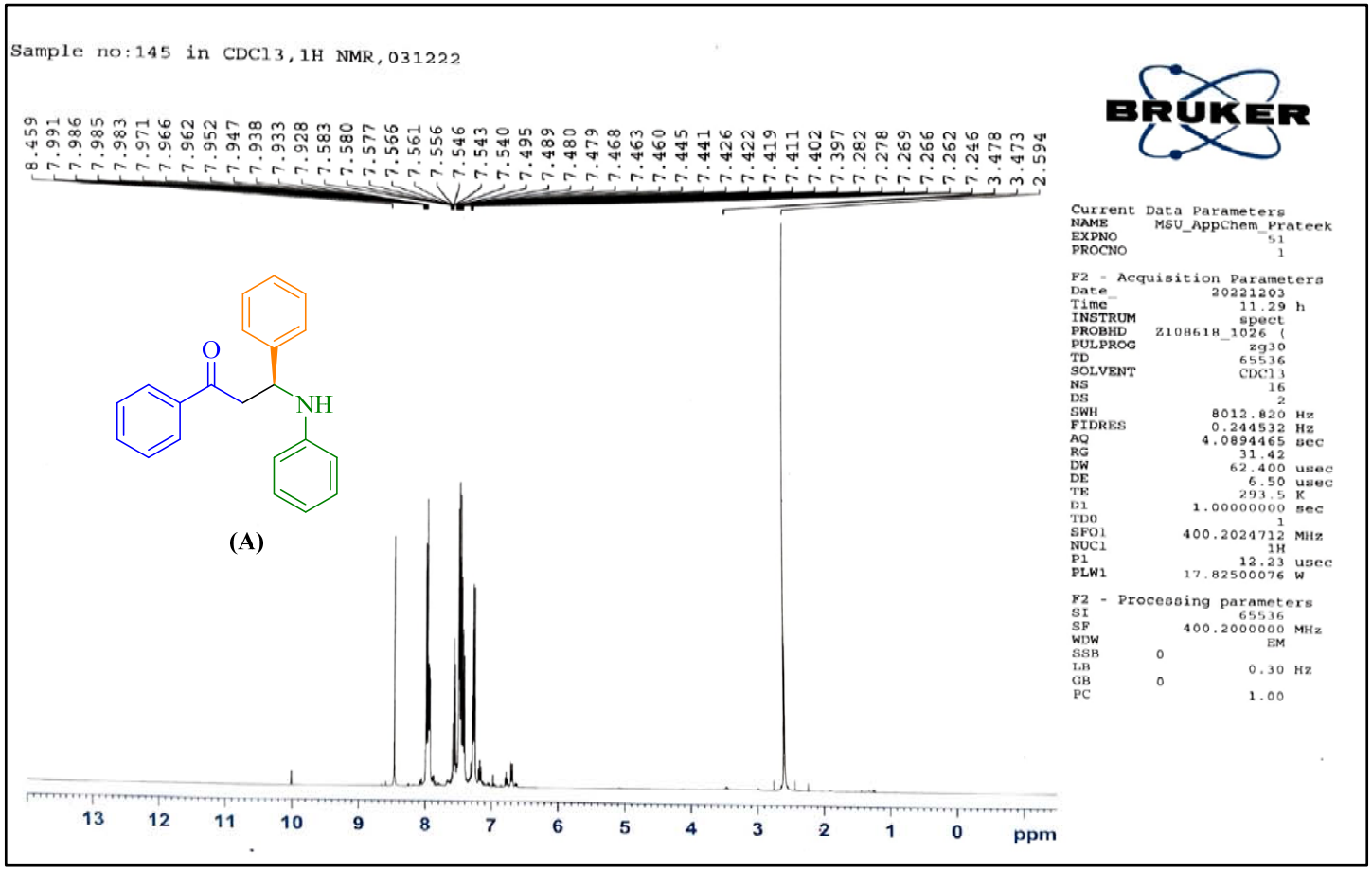

Fig. S26. ^{1}H NMR spectra of the product (A).

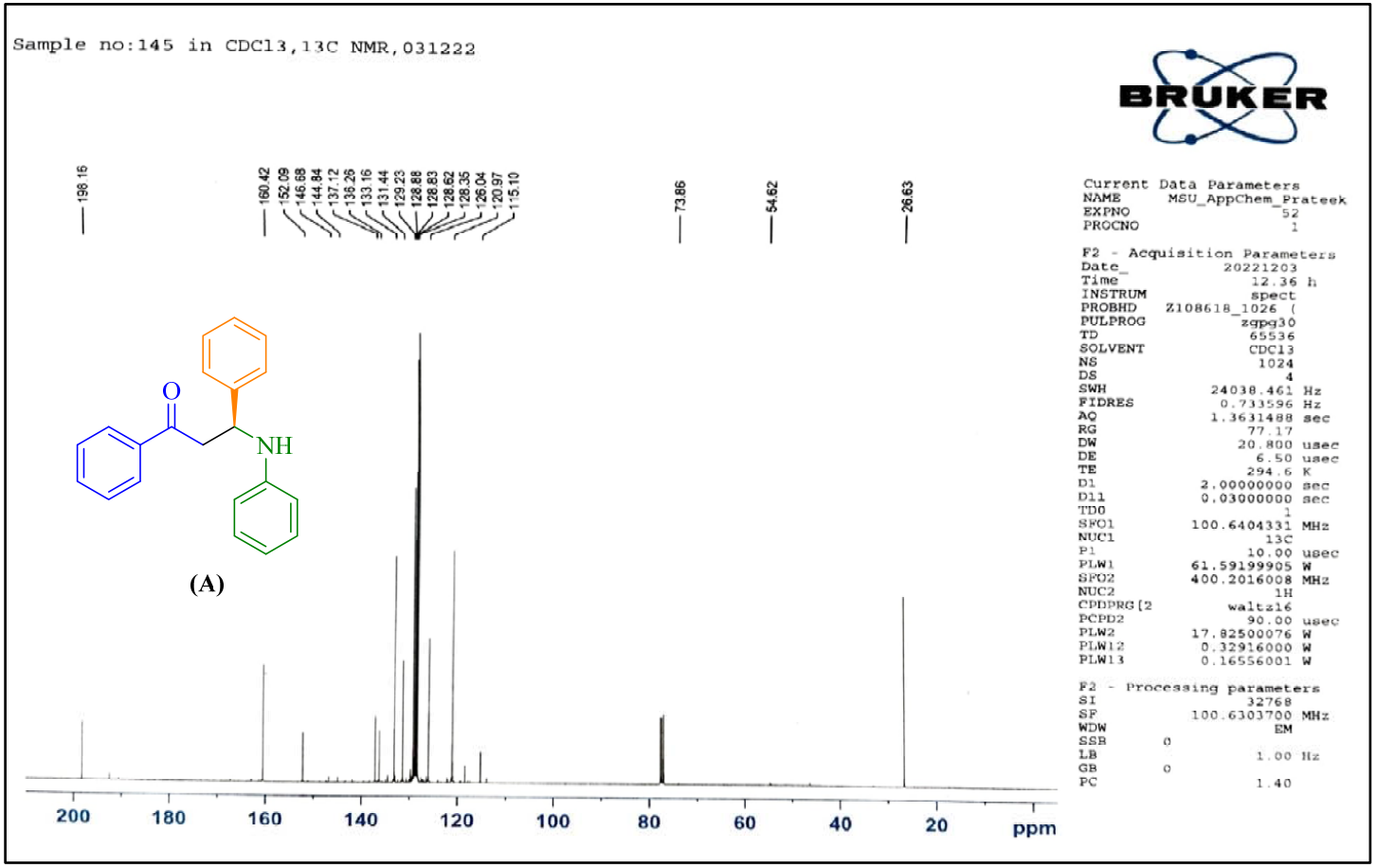

Fig. S27. ^{13}C NMR spectra of the product (A).

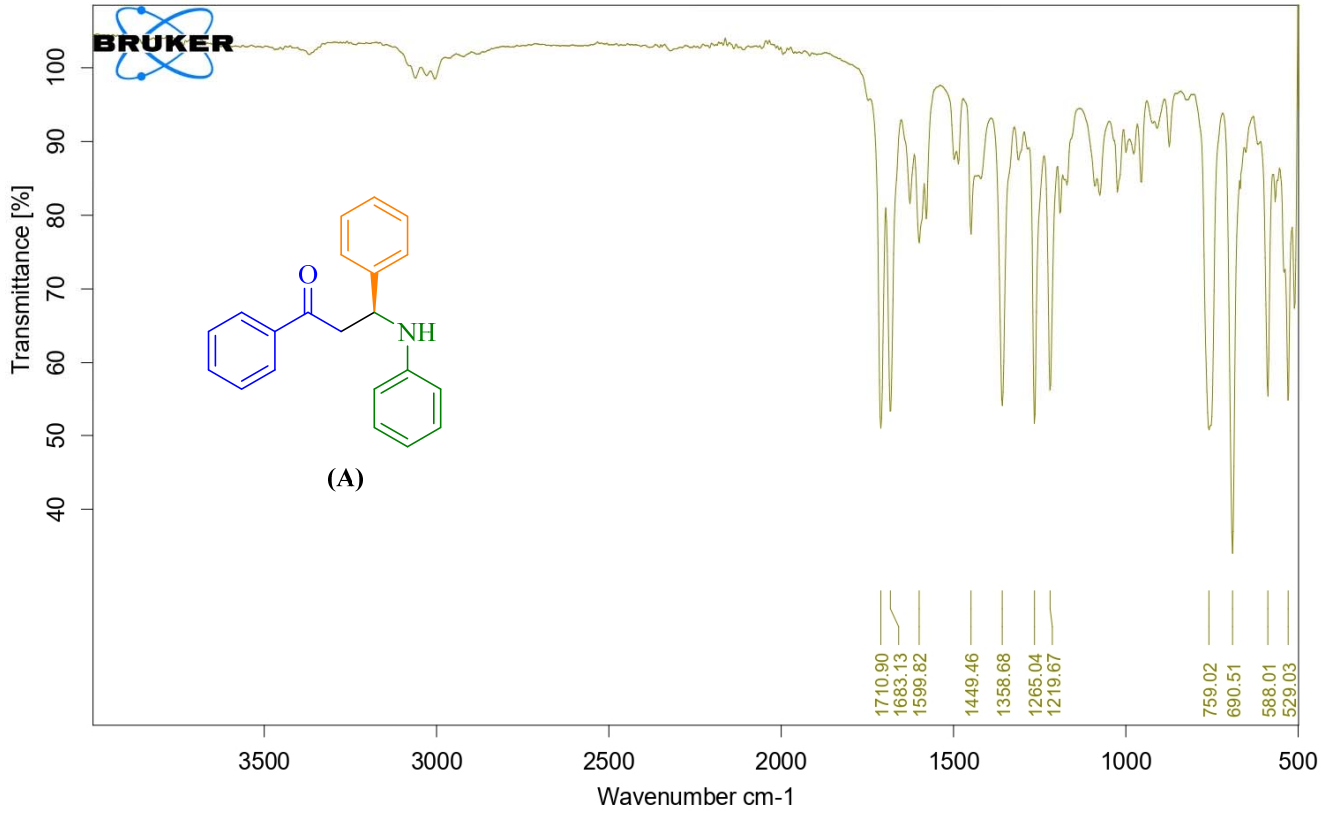

Fig. S28. FTIR spectra of the product (A).

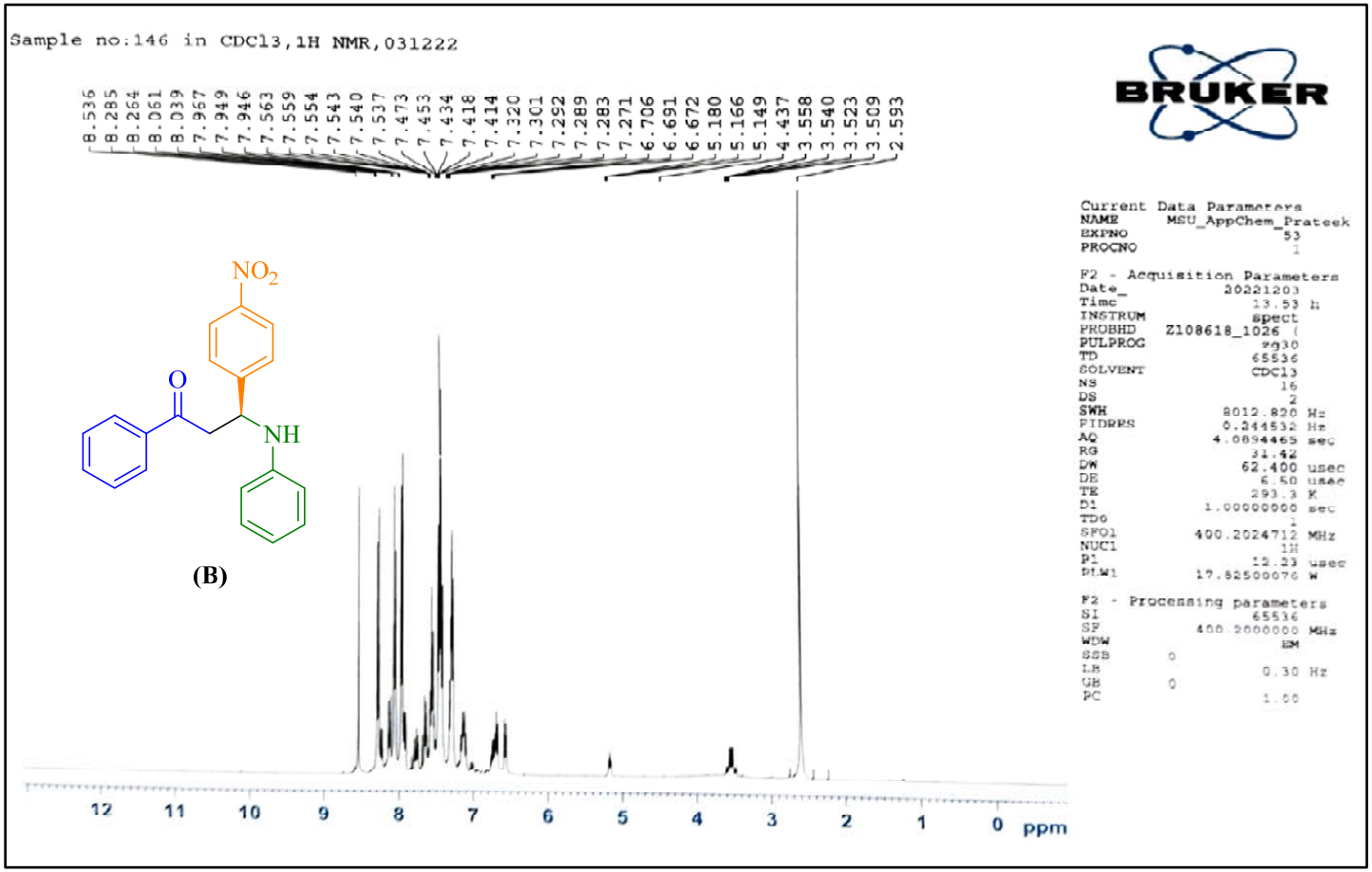

Fig. S29. ^{1}H NMR spectra of the product (B).

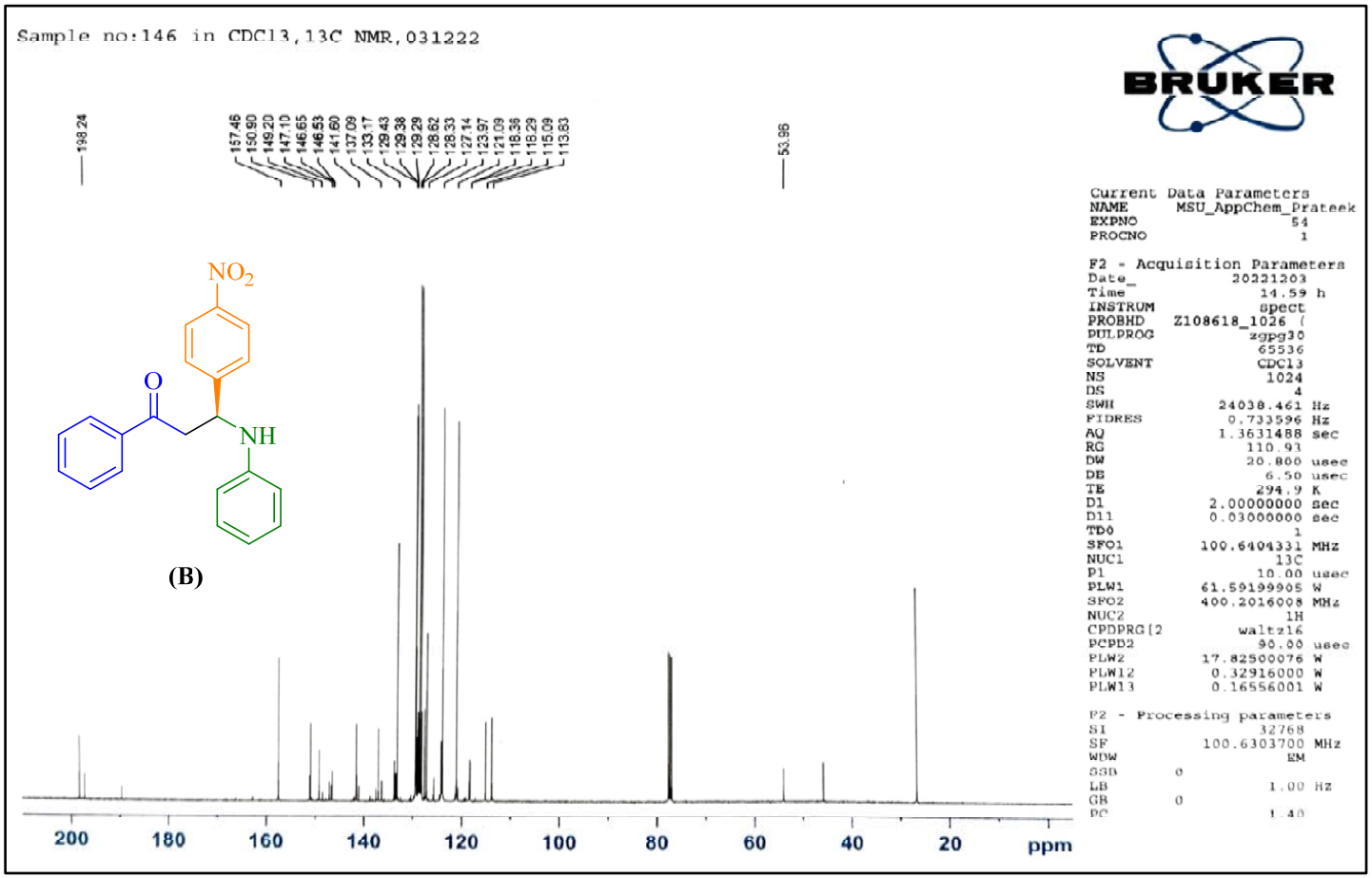

Fig. S30. ^{13}C NMR spectra of the product (B).

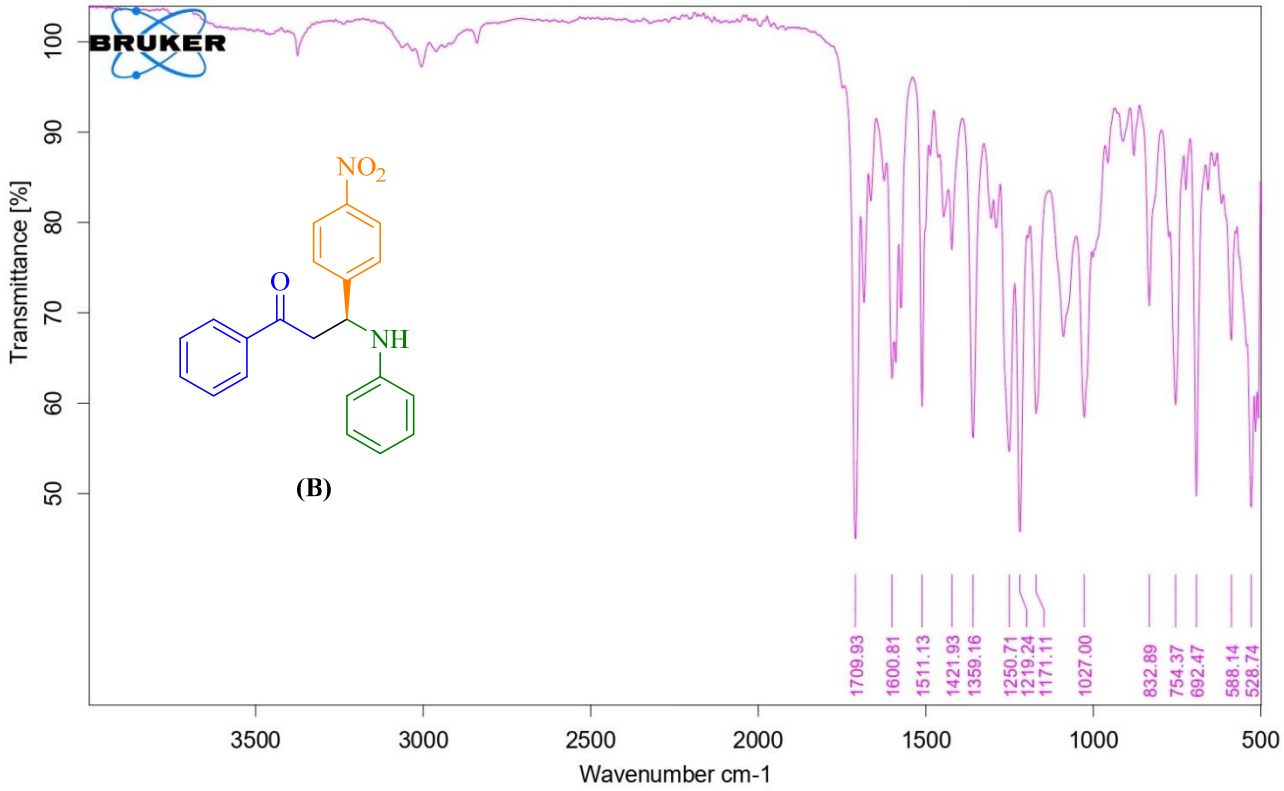

Fig. S31. FTIR spectra of the product (B).

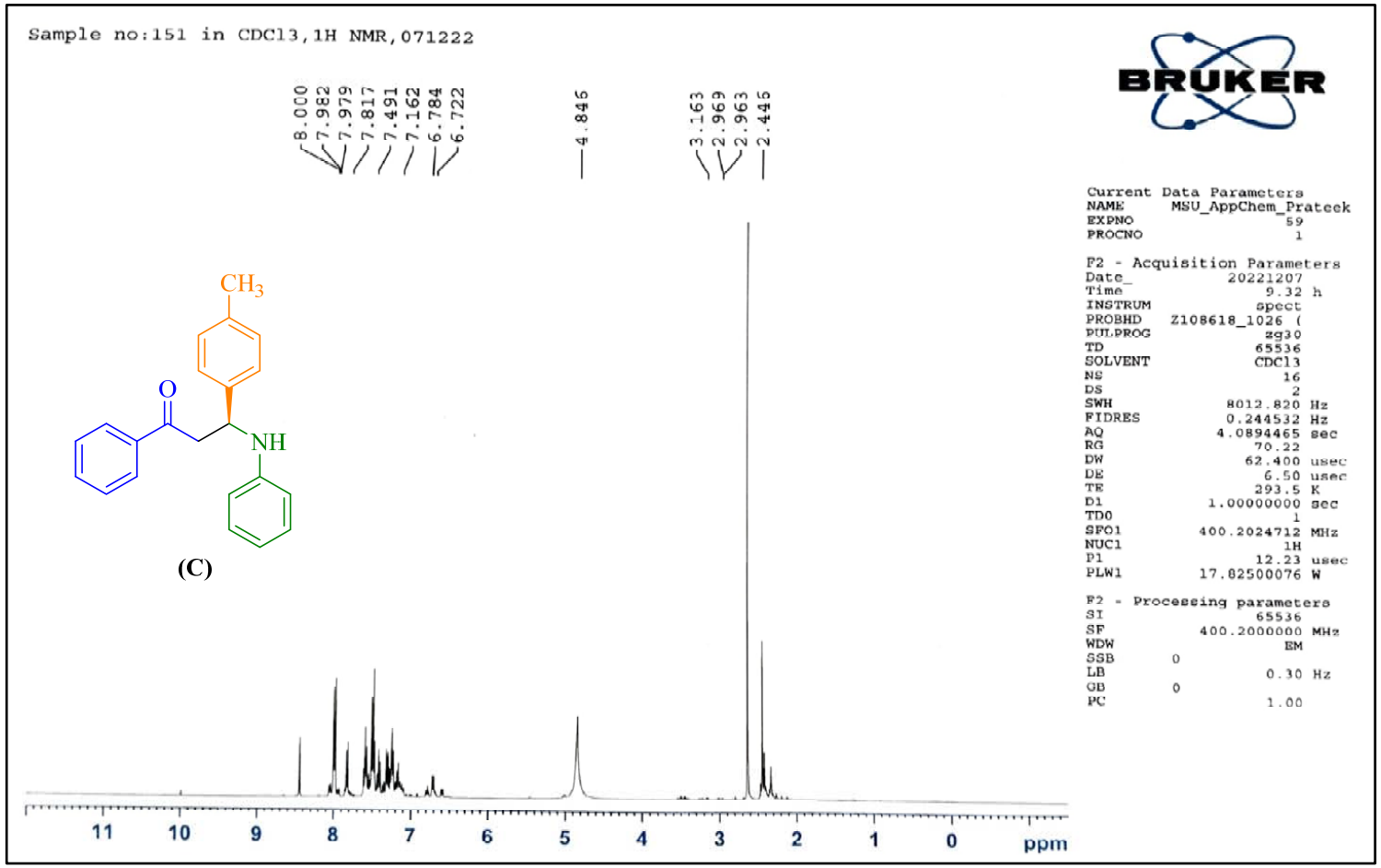

Fig. S32. ^{1}H NMR spectra of the product (C).

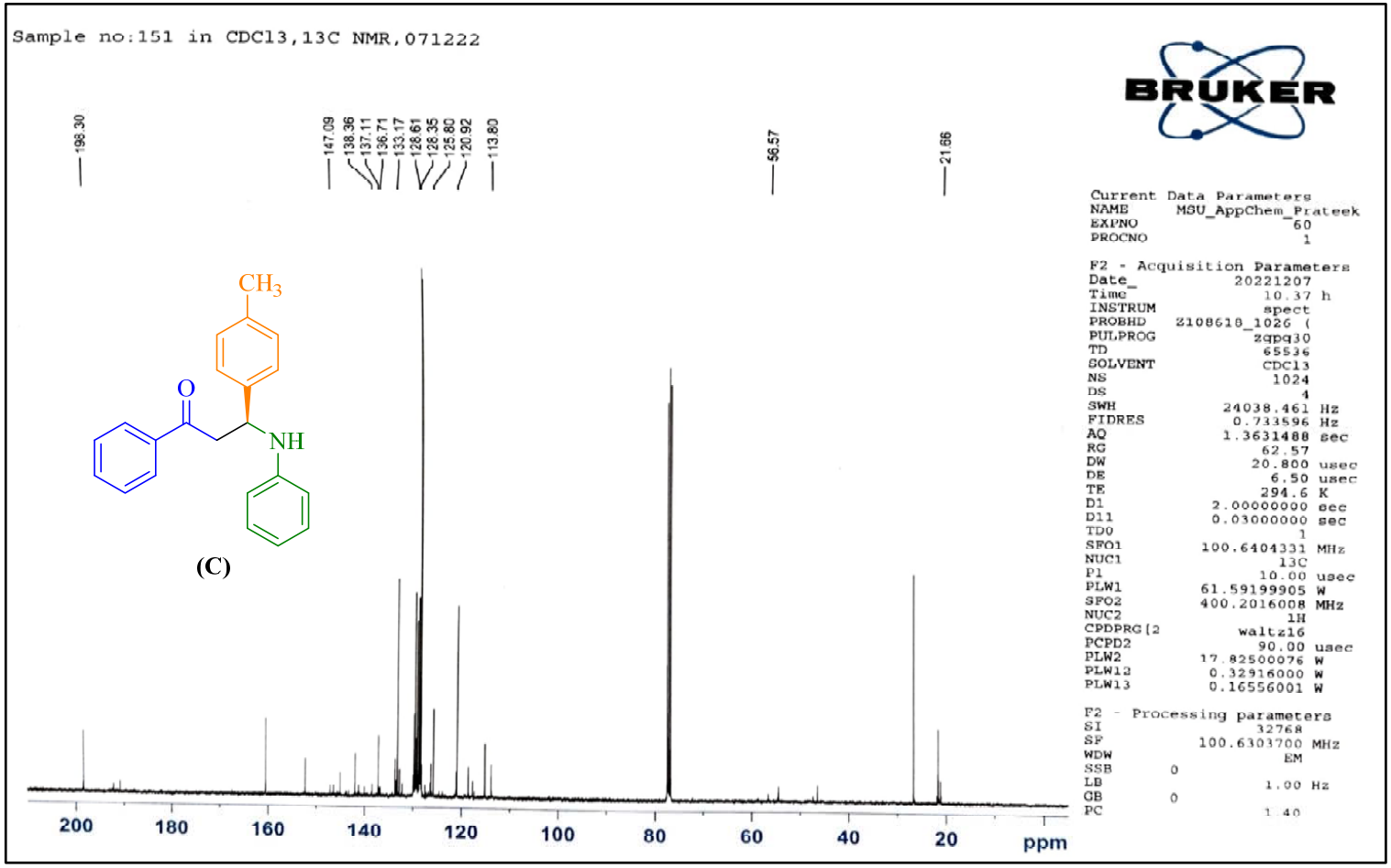

Fig. S33. ^{13}C NMR spectra of the product (C).

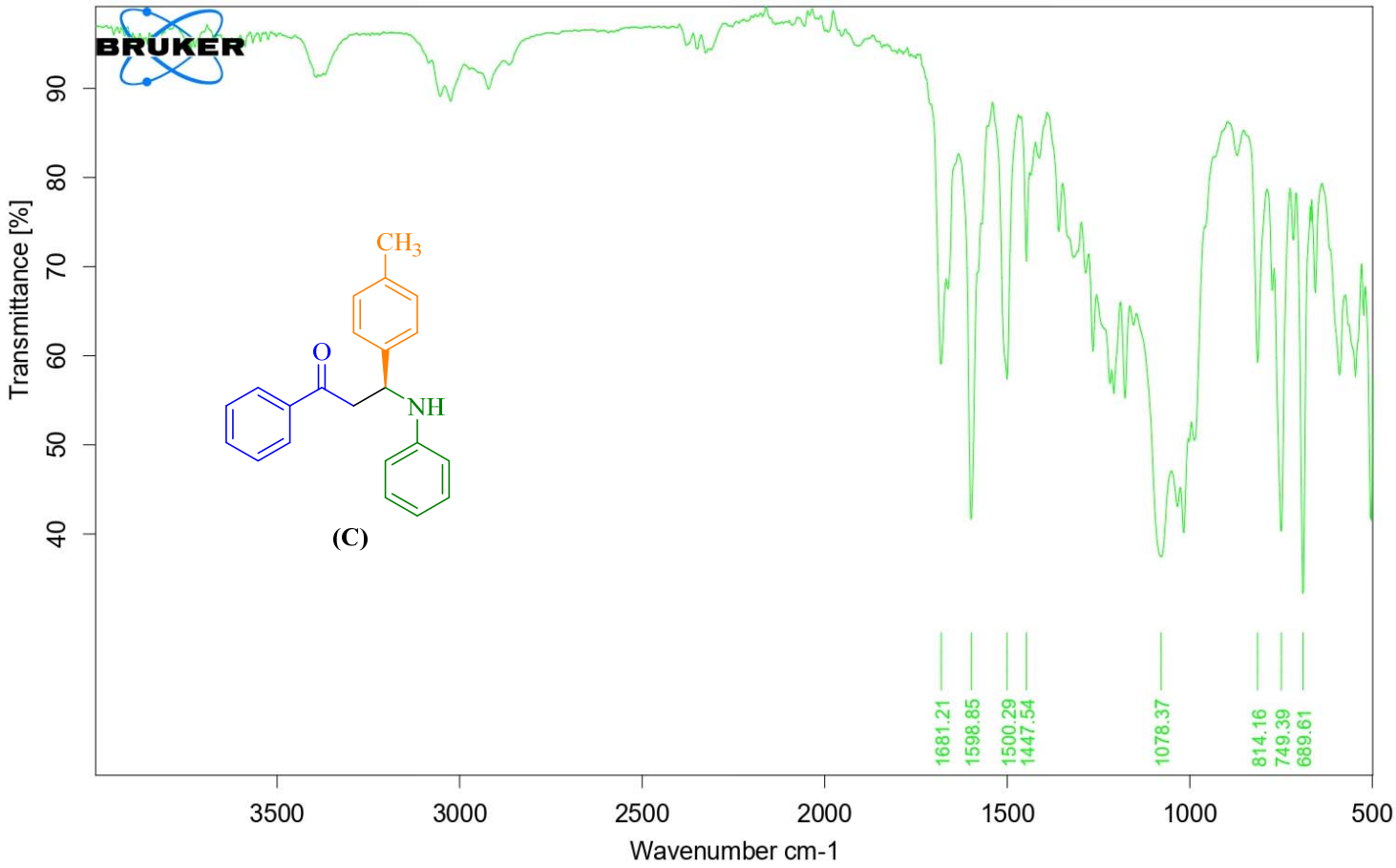

Fig. S34. FTIR spectra of the product (C).

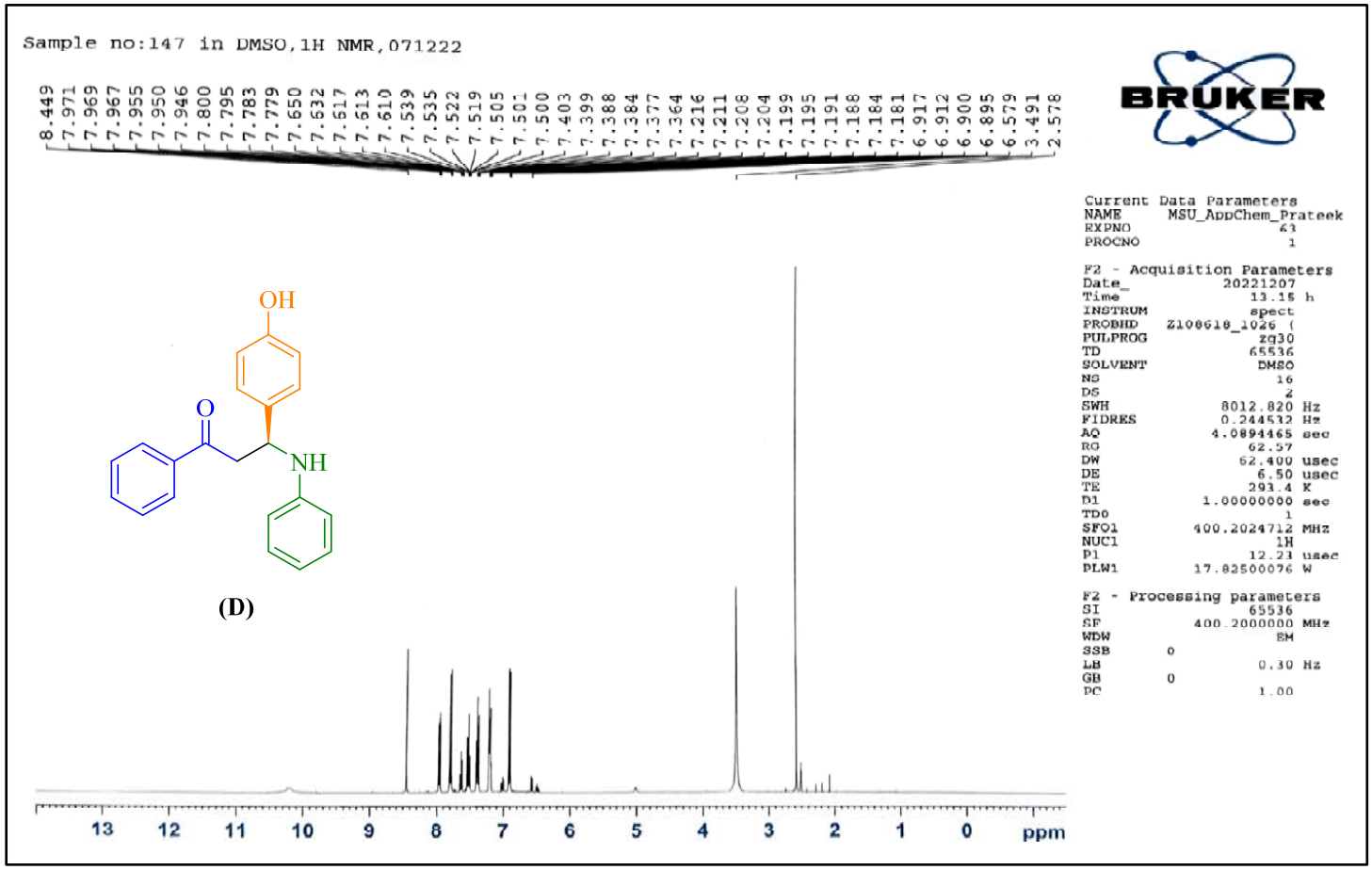

Fig. S35. ^{1}H NMR spectra of the product (D).

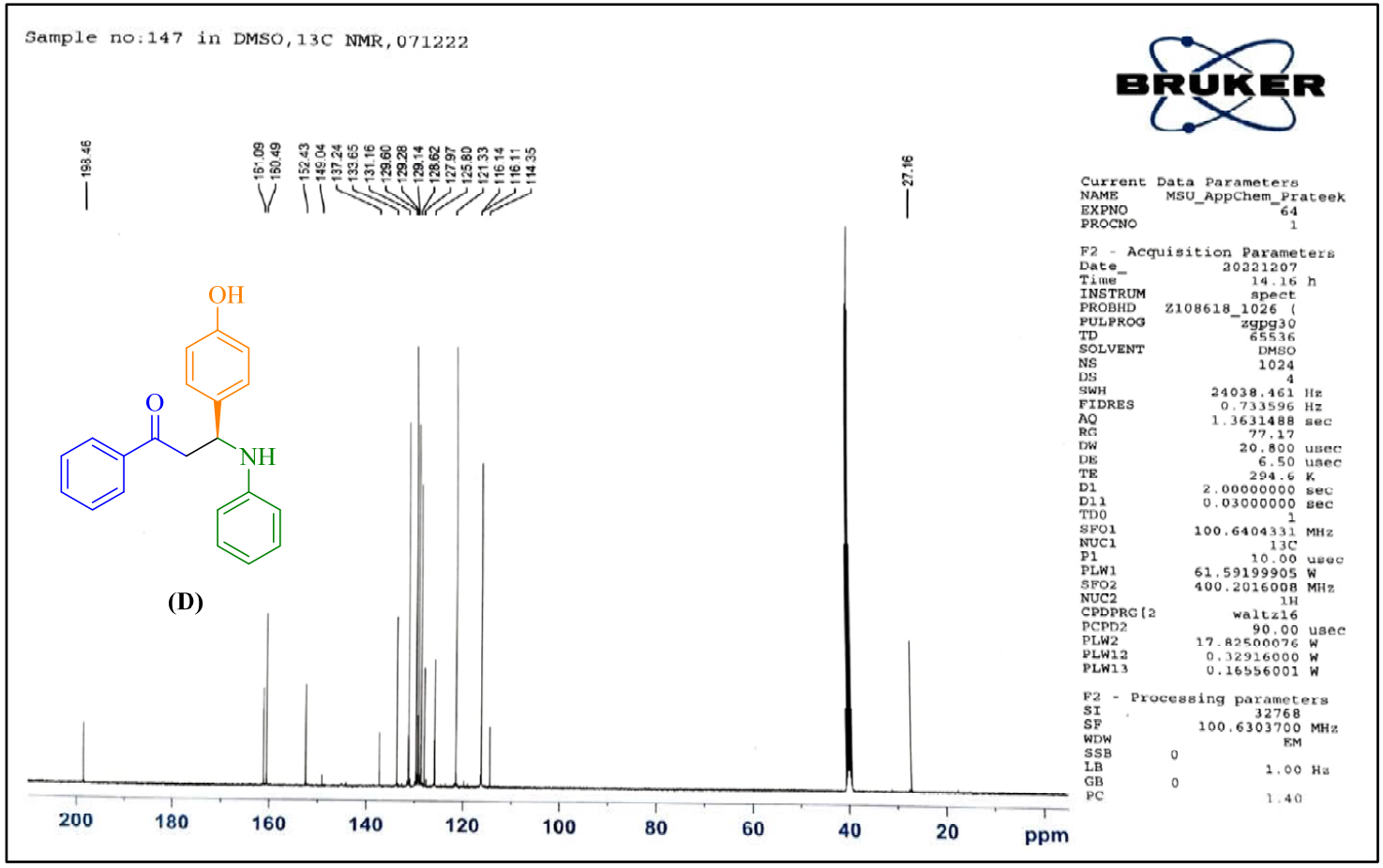

Fig. S36. ^{13}C NMR spectra of the product (D).

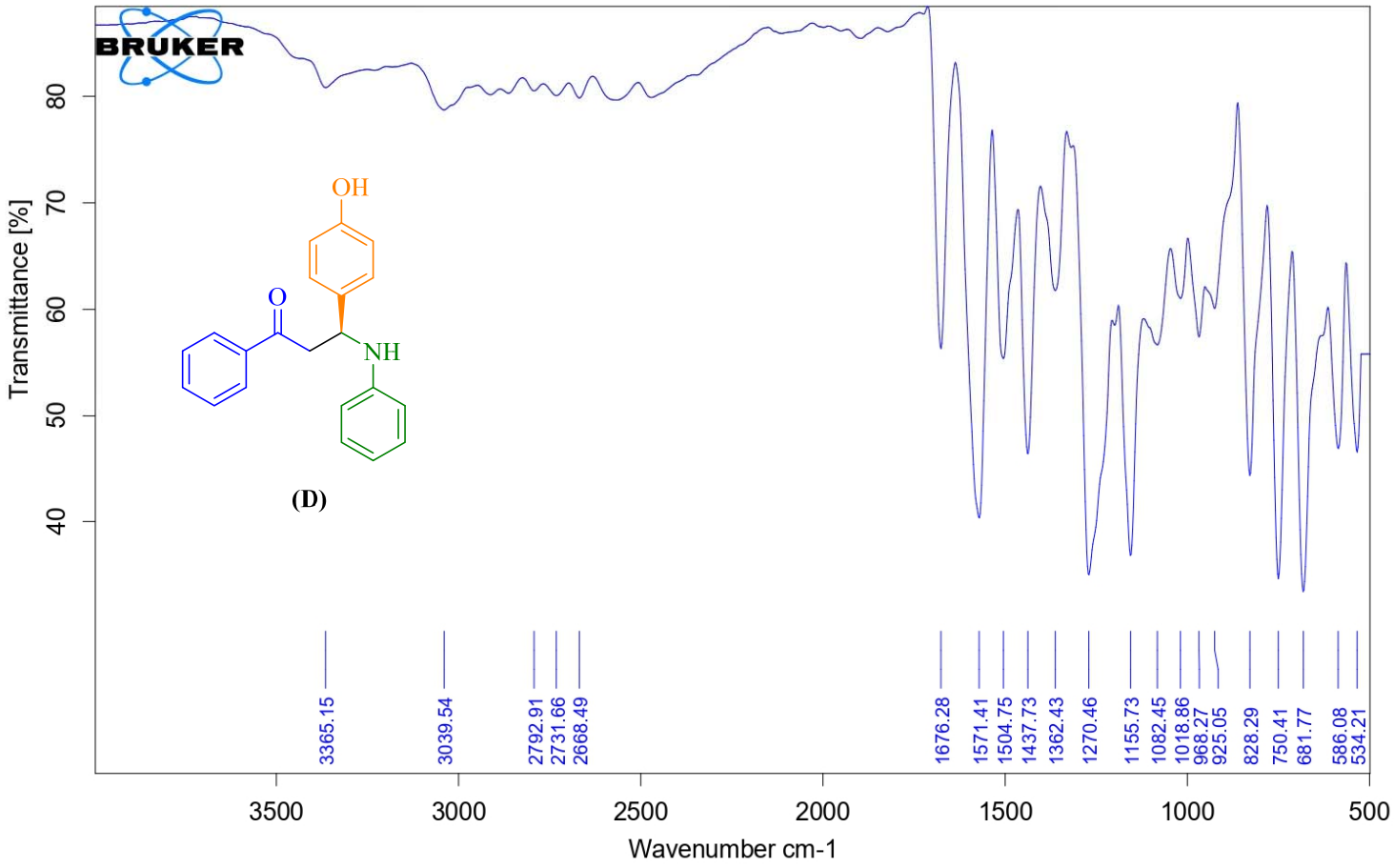

Fig. S37. FTIR spectra of the product (D).

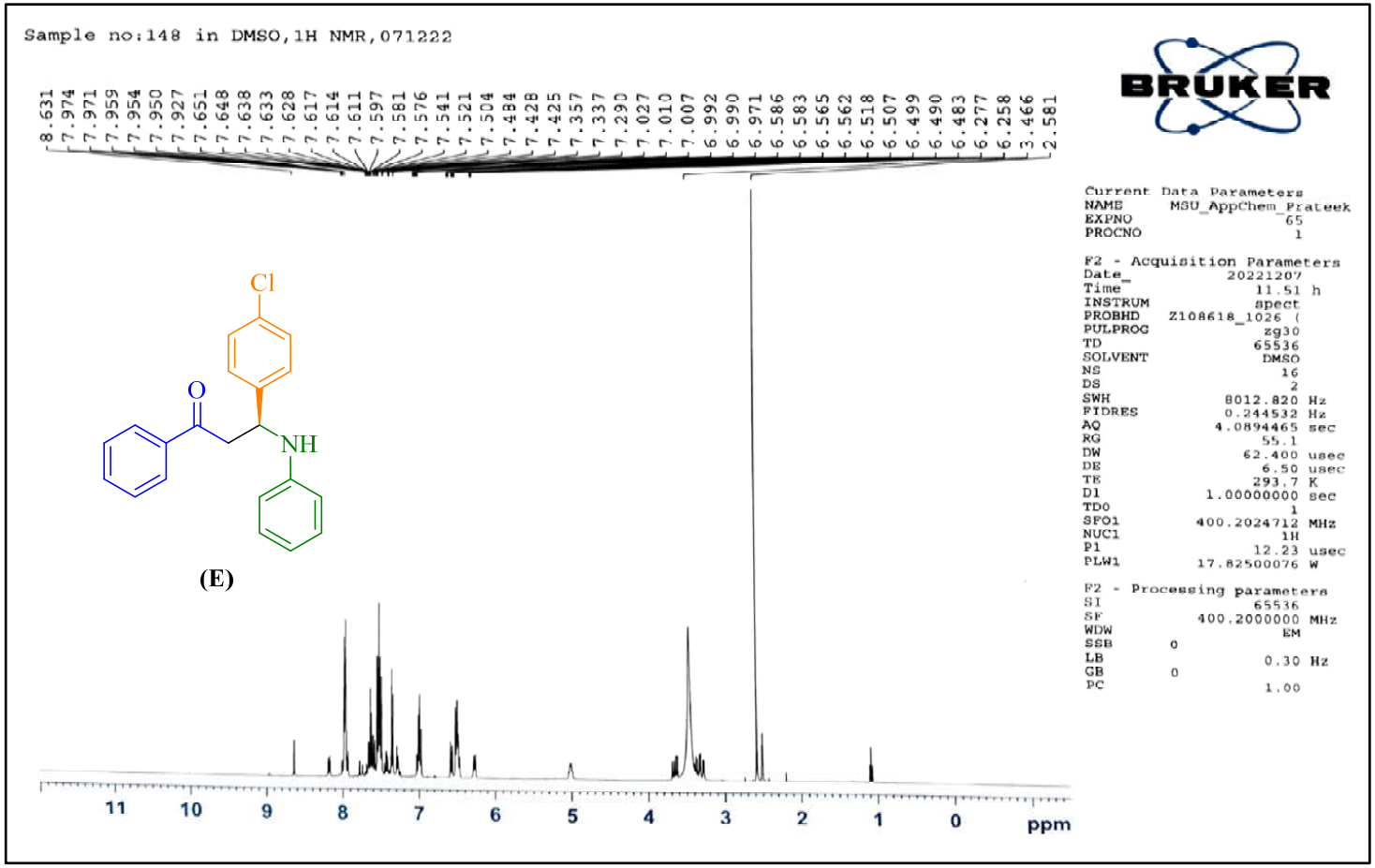

Fig. S38. ^{1}H NMR spectra of the product (E).

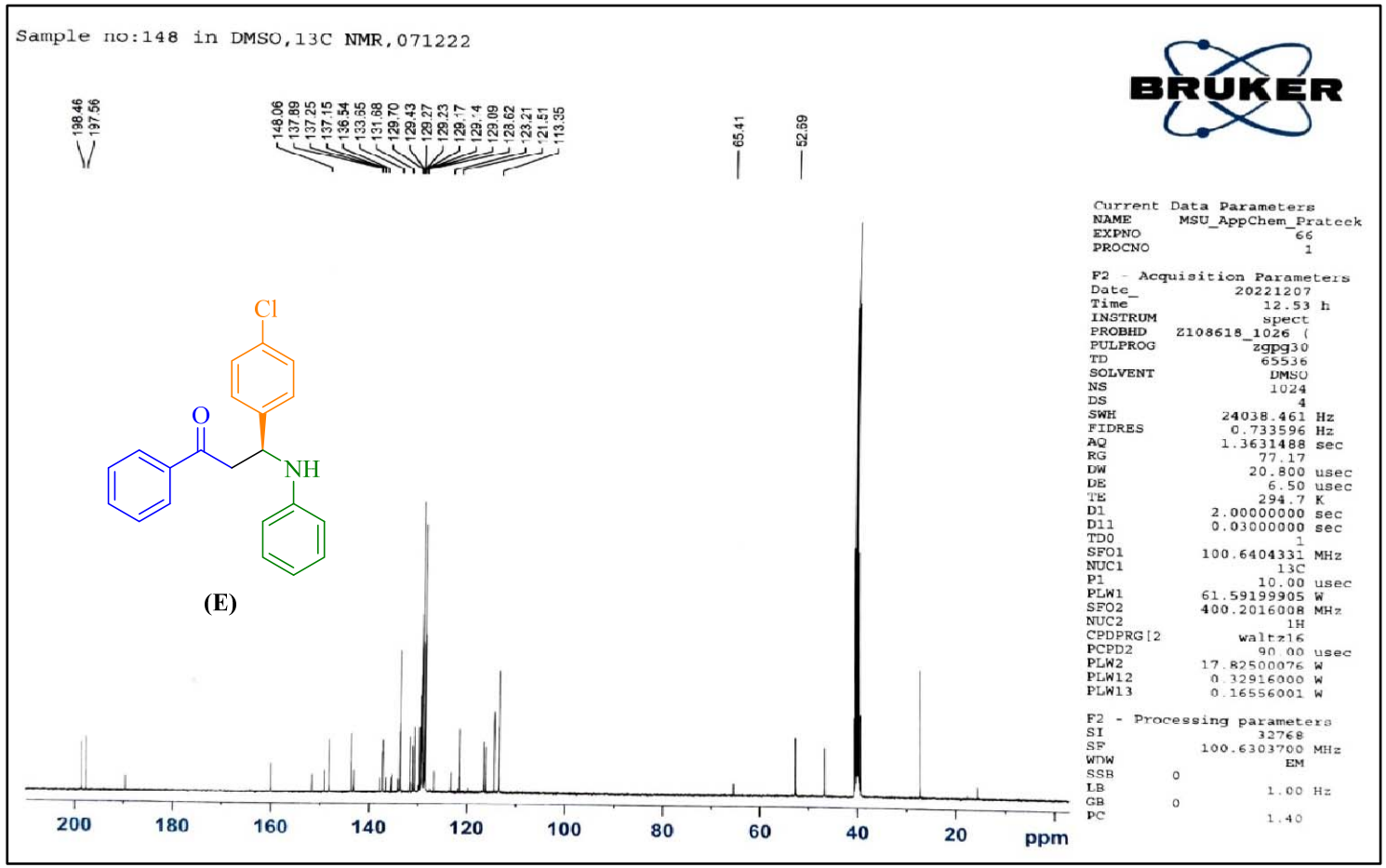

Fig. S39. ^{13}C NMR spectra of the product (E).

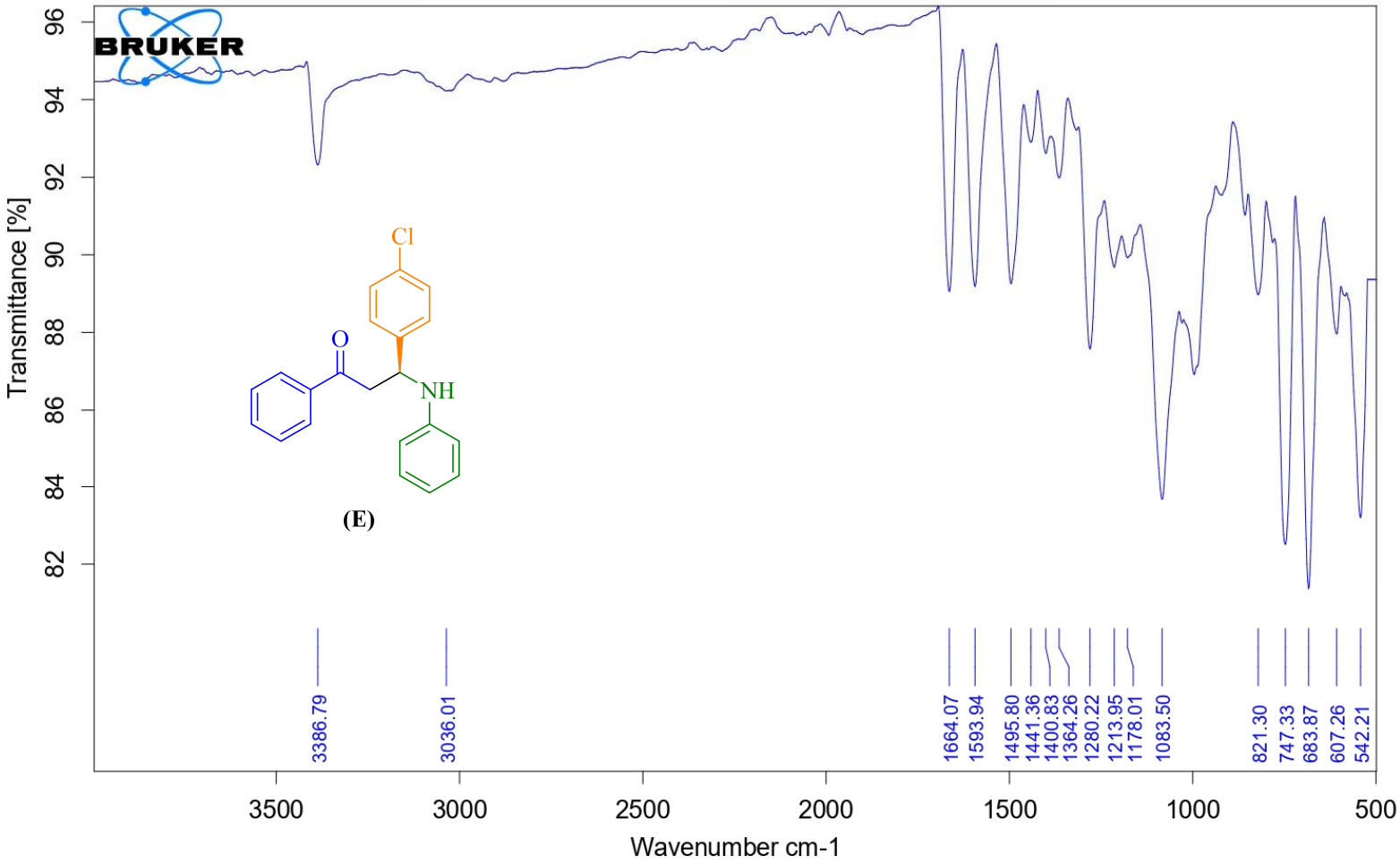

Fig. S40. FTIR spectra of the product (E).

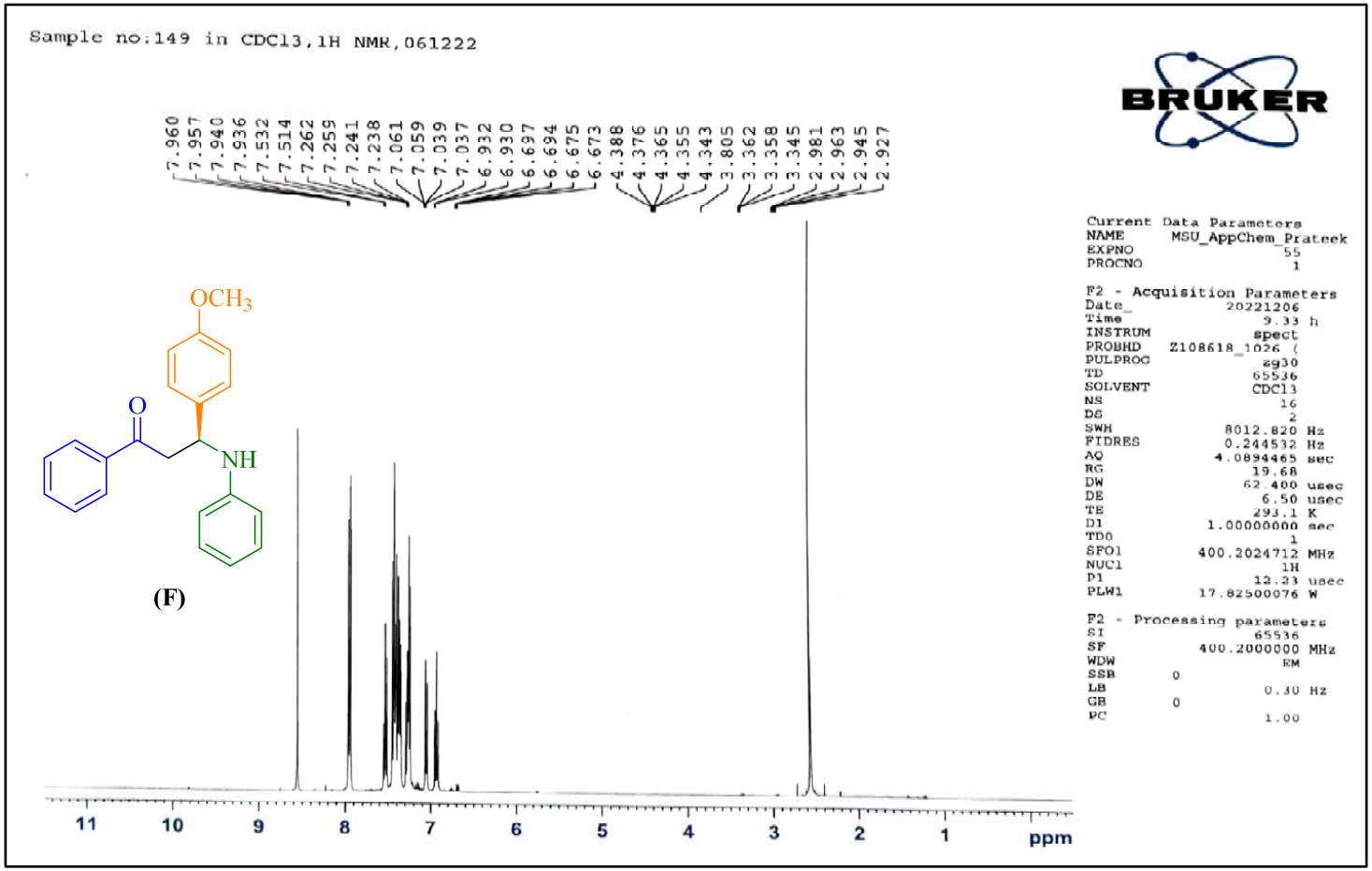

Fig. S41. ^{1}H NMR spectra of the product (F).

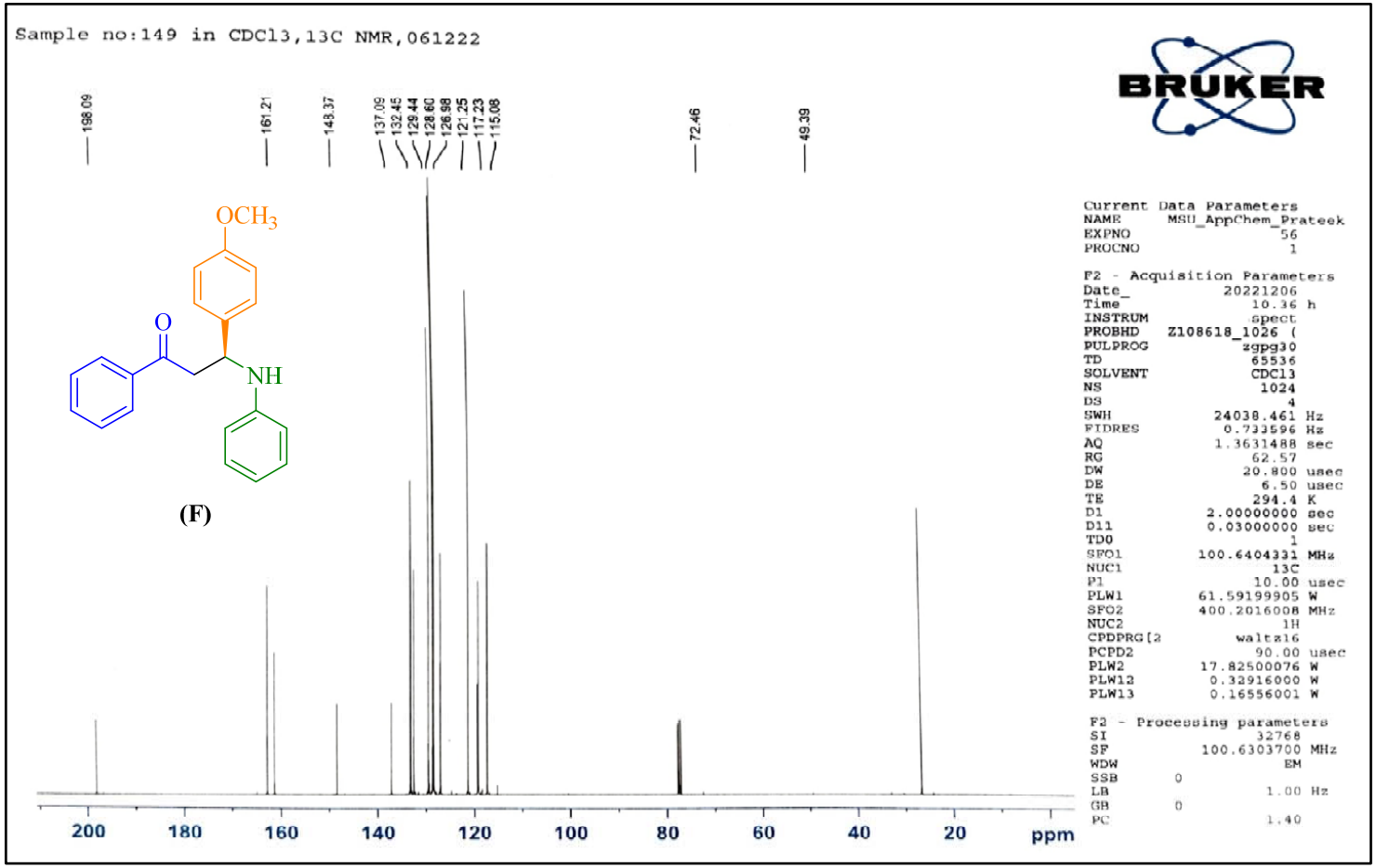

Fig. S42. ^{13}C NMR spectra of the product (F).

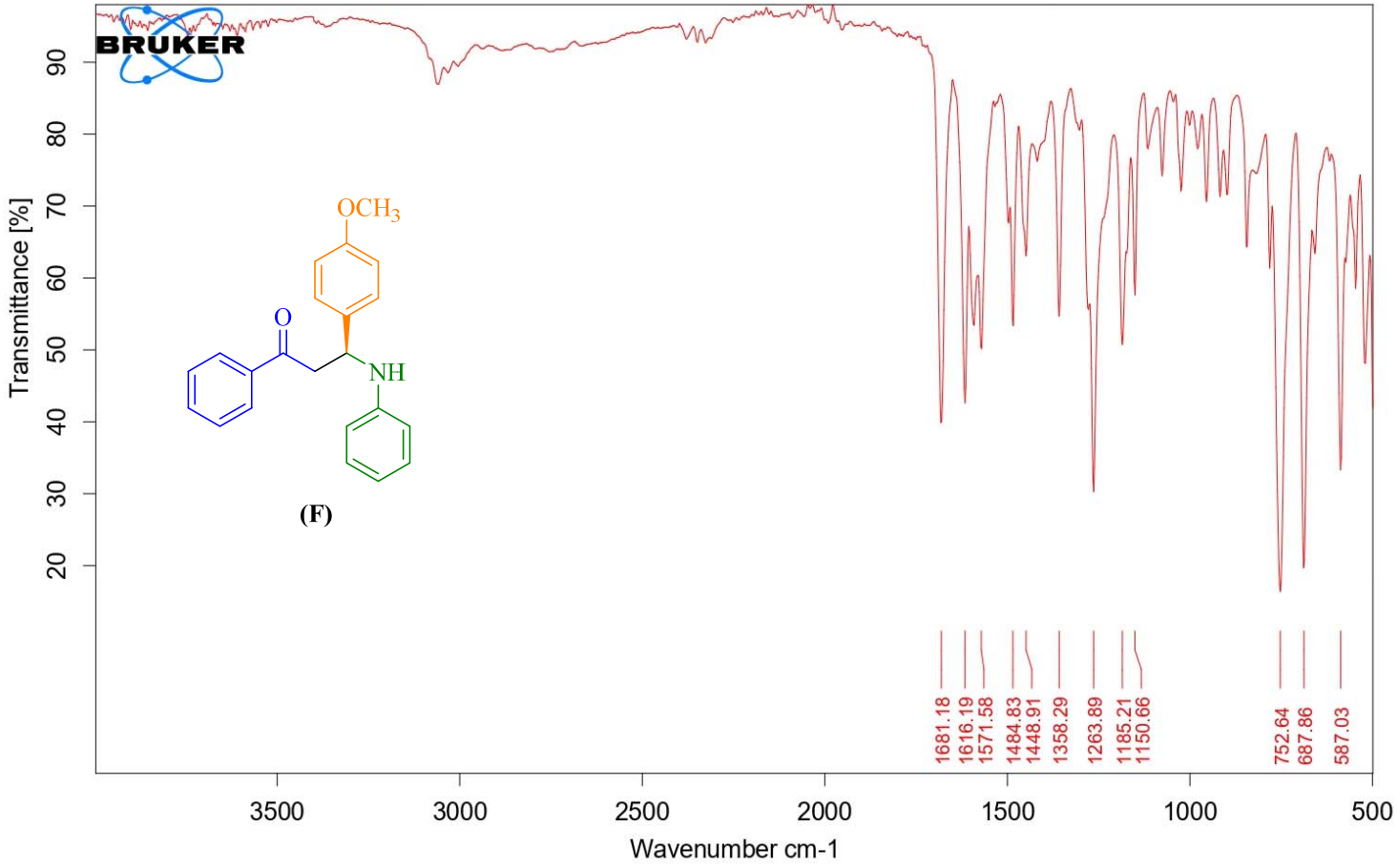

Fig. S43. FTIR spectra of the product (F).

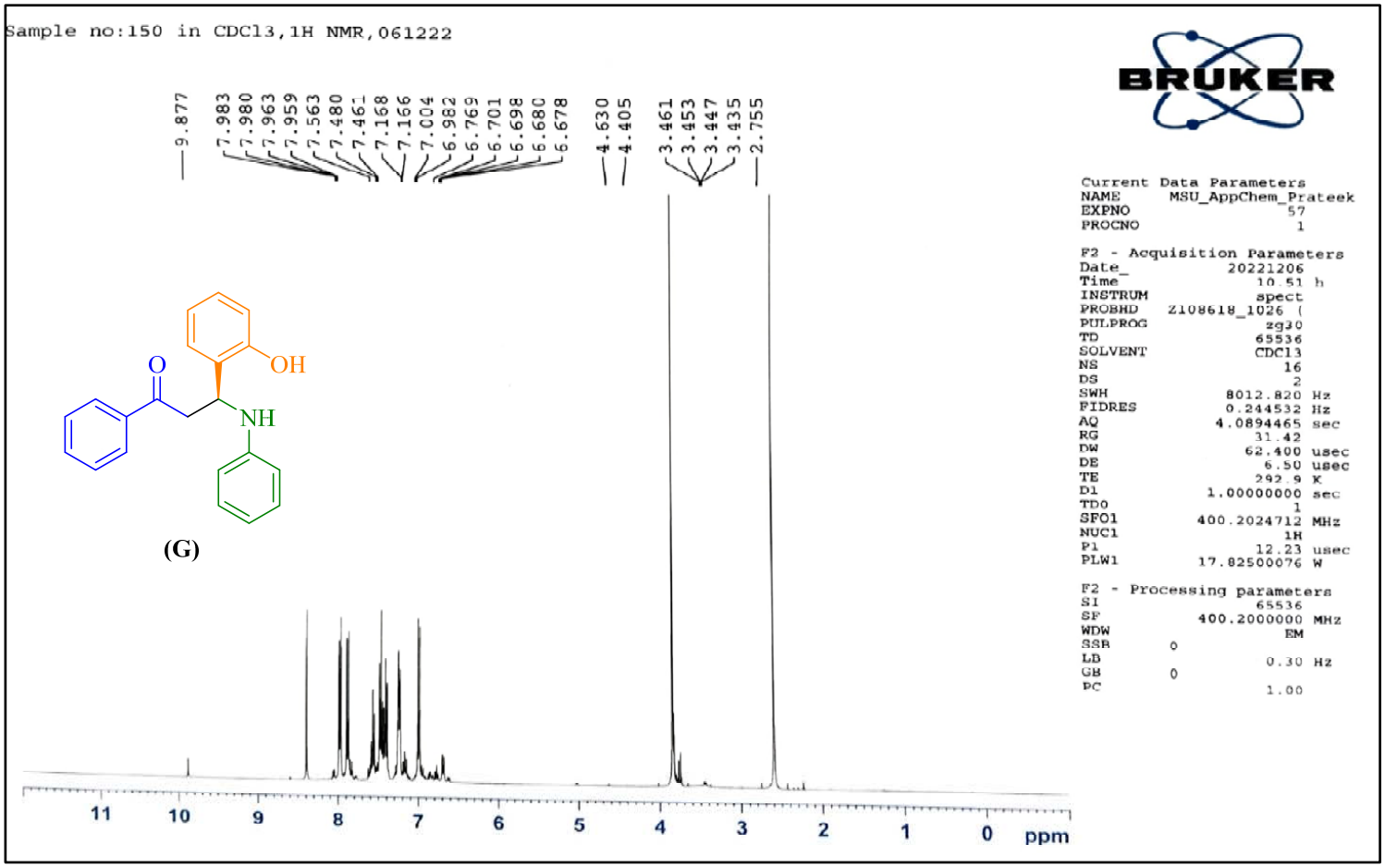

Fig. S44. ^{1}H NMR spectra of the product (G).

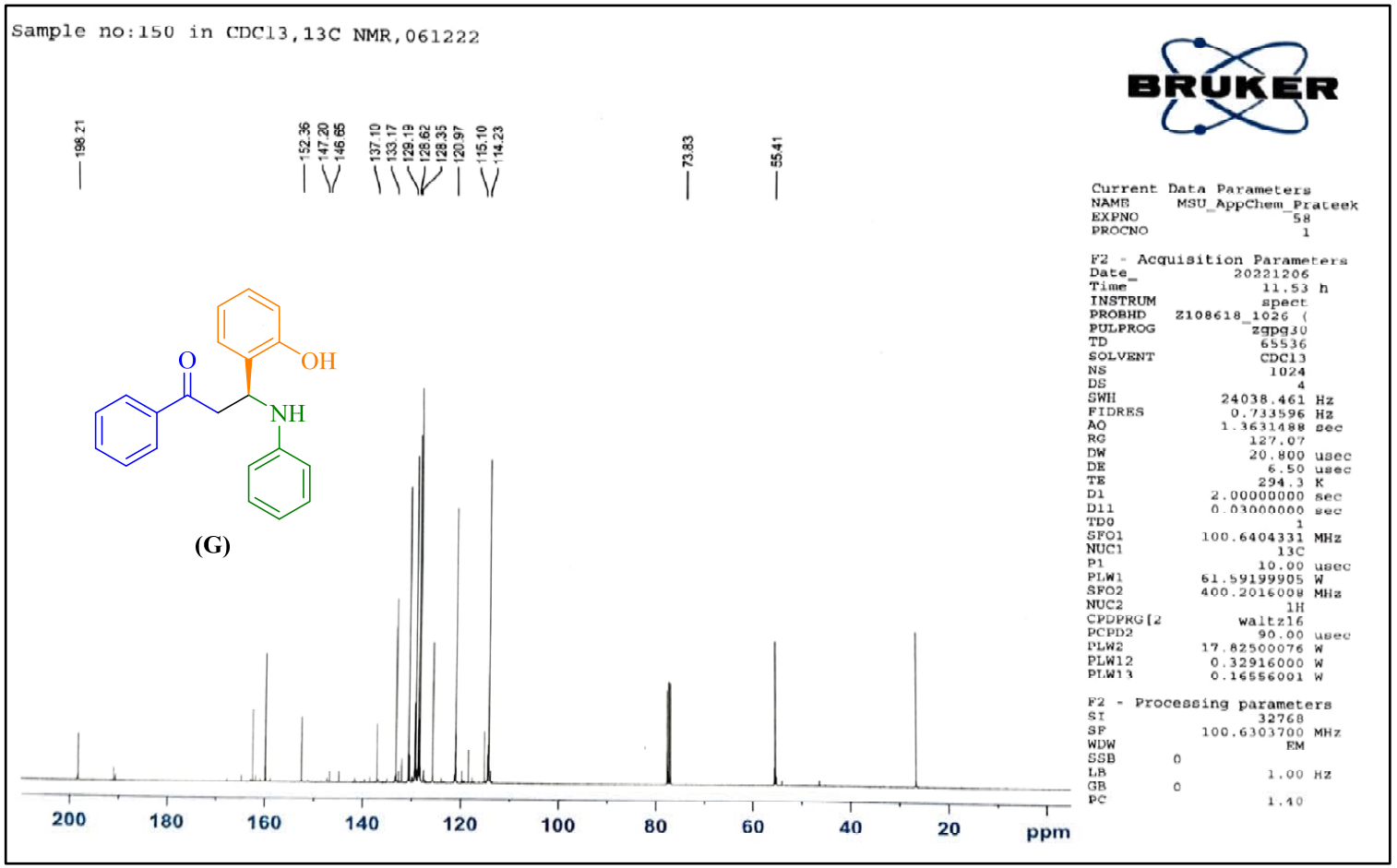

Fig. S45. ^{13}C NMR spectra of the product (G).

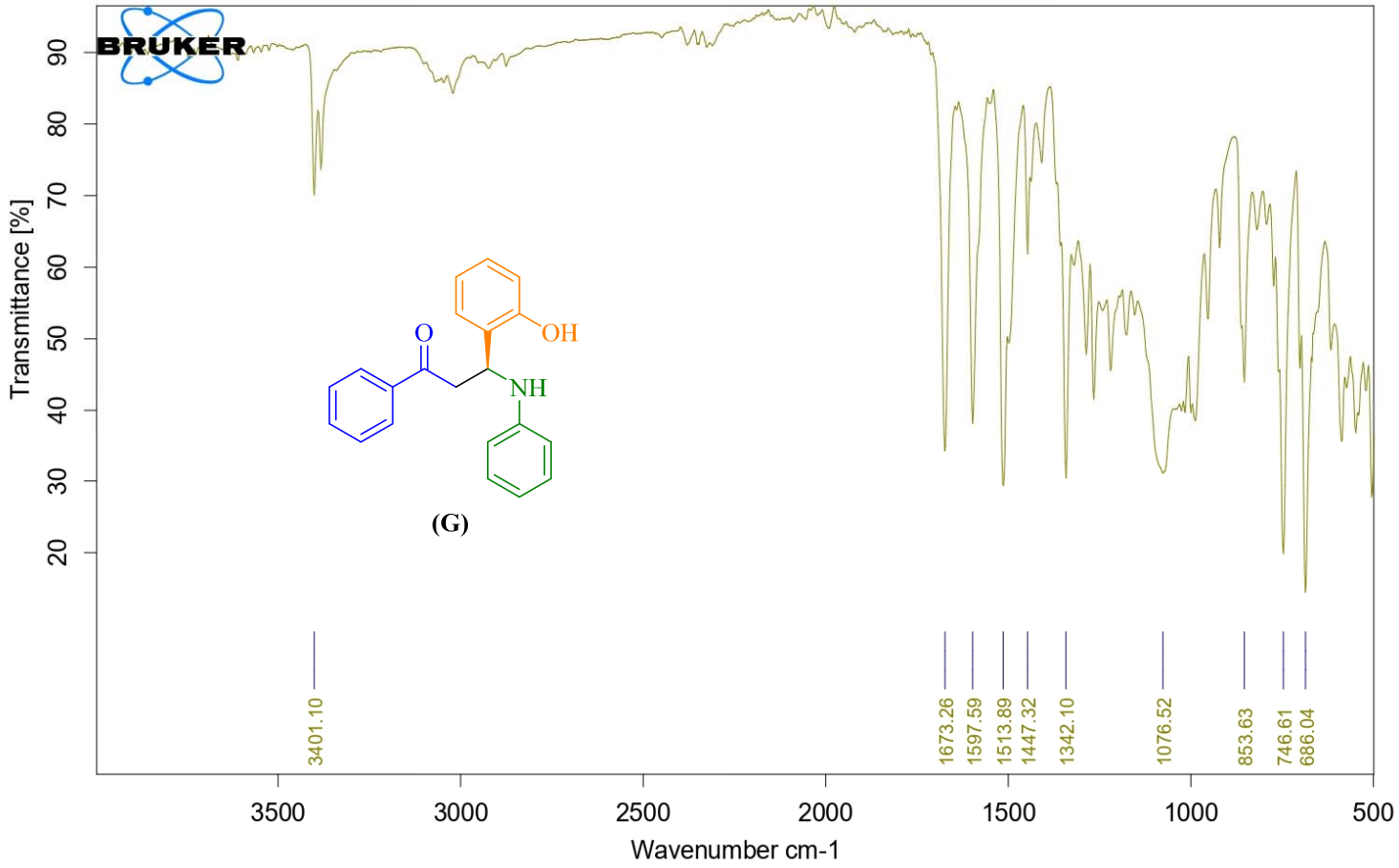

Fig. S46. FTIR spectra of the product (G).

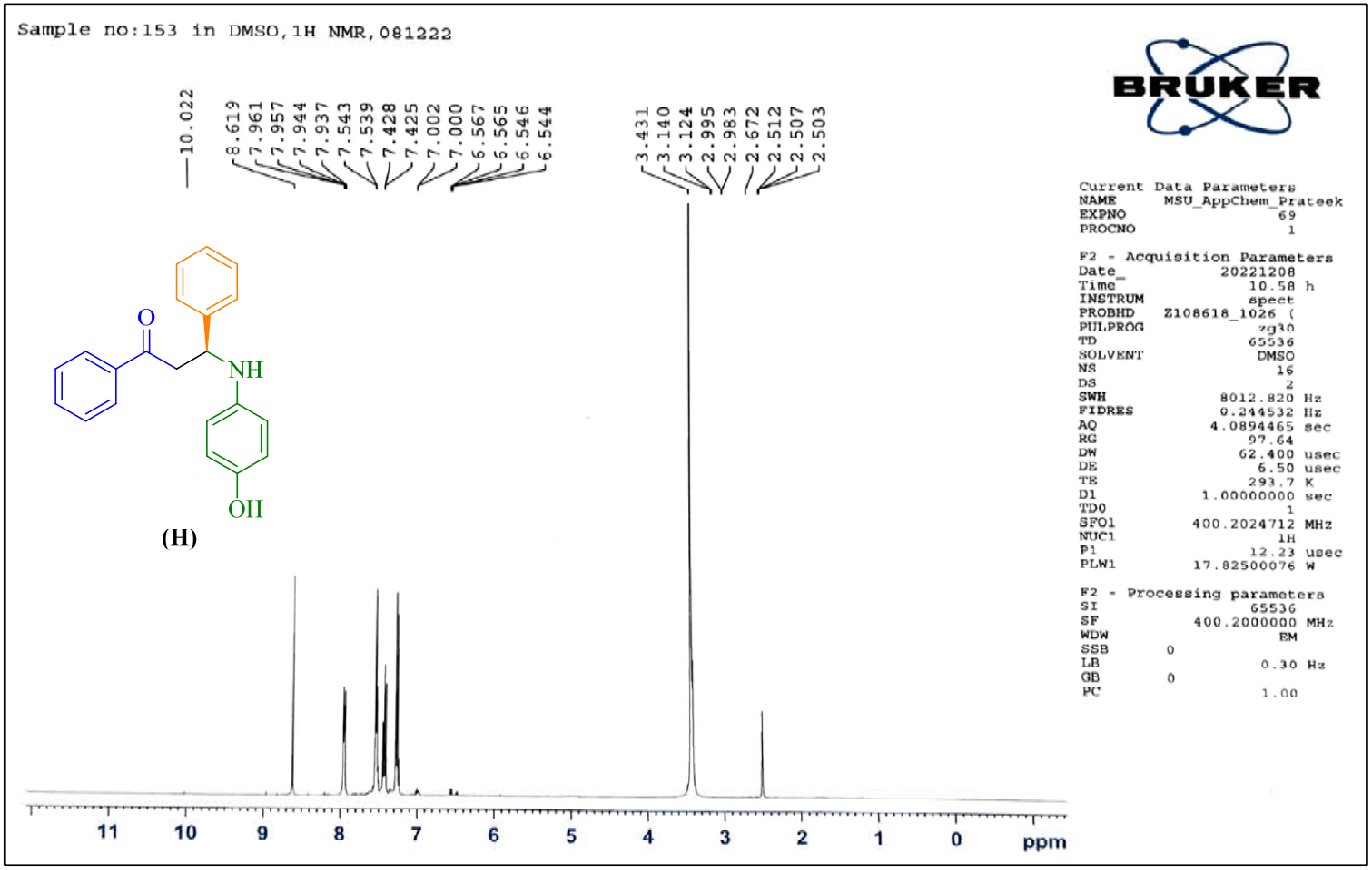

Fig. S47. ^{1}H NMR spectra of the product (H).

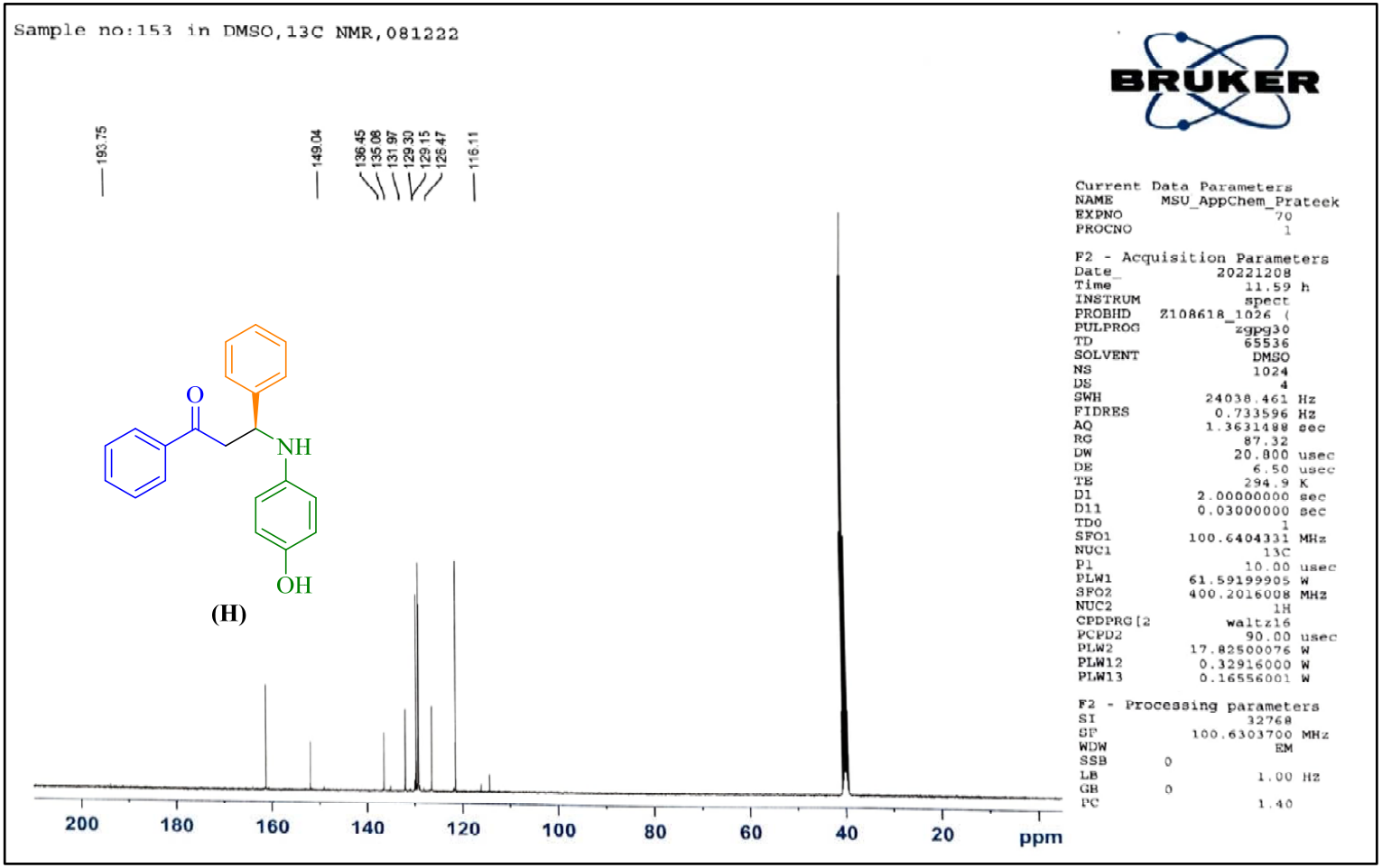

Fig. S48. ^{13}C NMR spectra of the product (H).

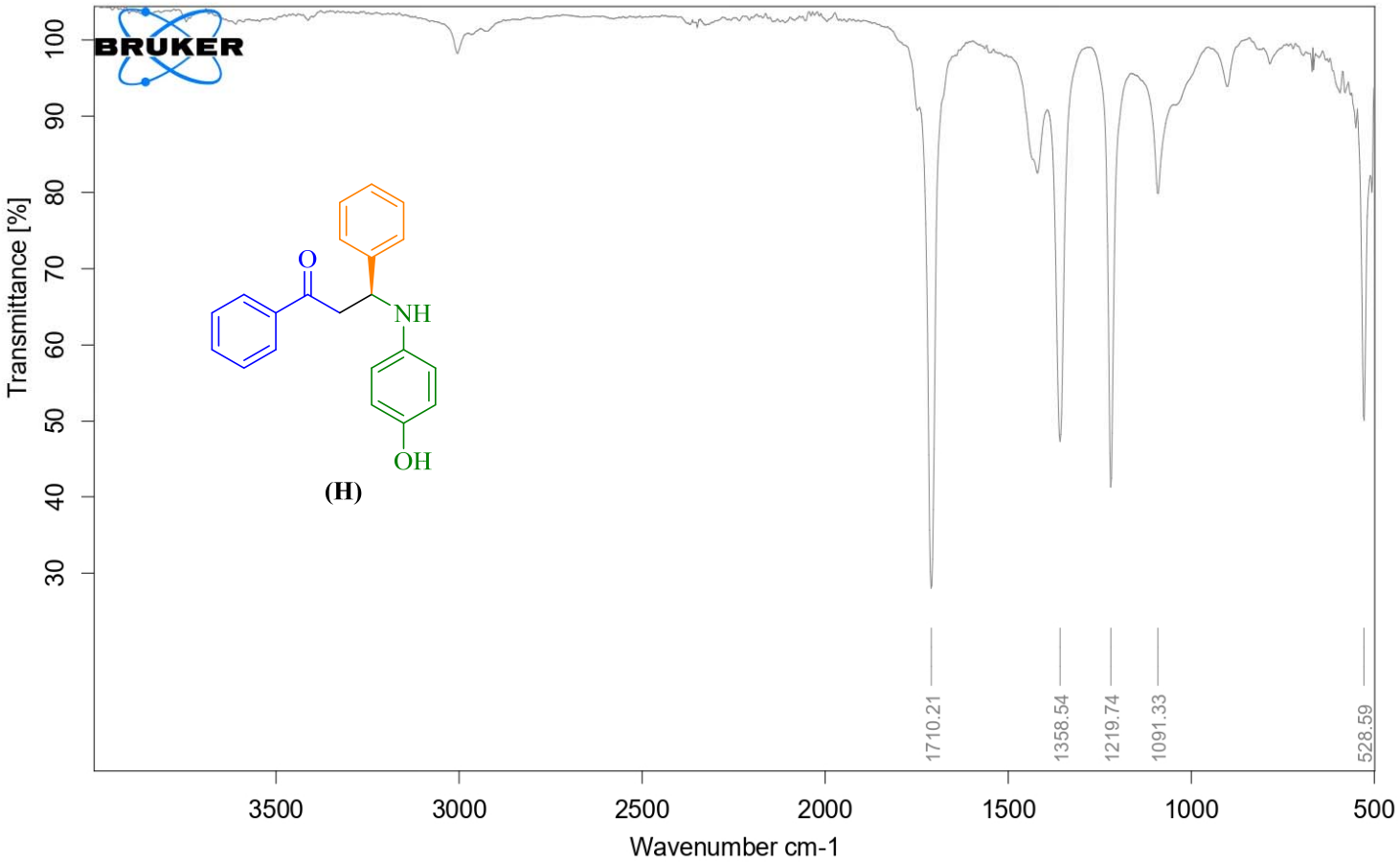

Fig. S49. FTIR spectra of the product (H).

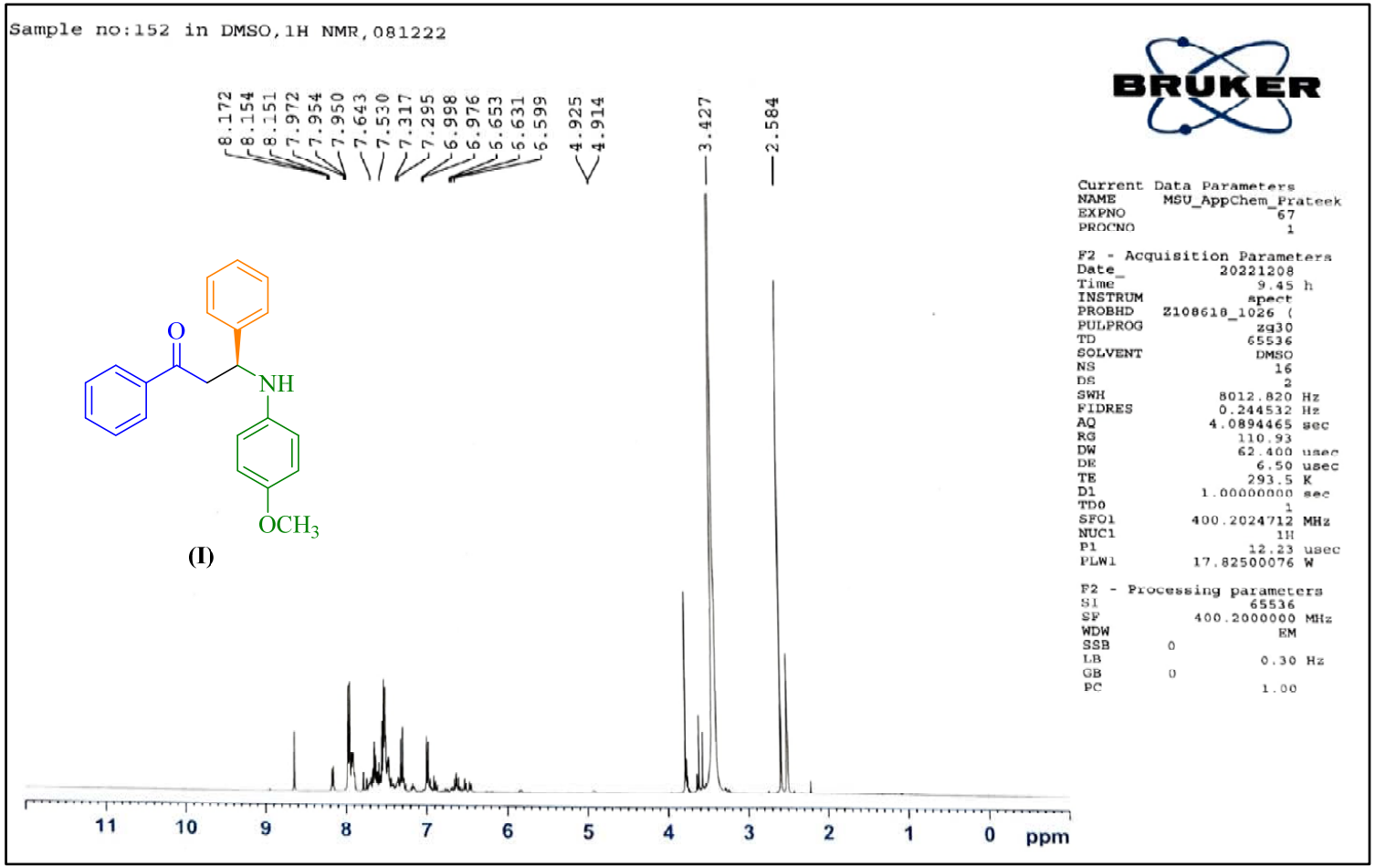

Fig. S50. ^{1}H NMR spectra of the product (I).

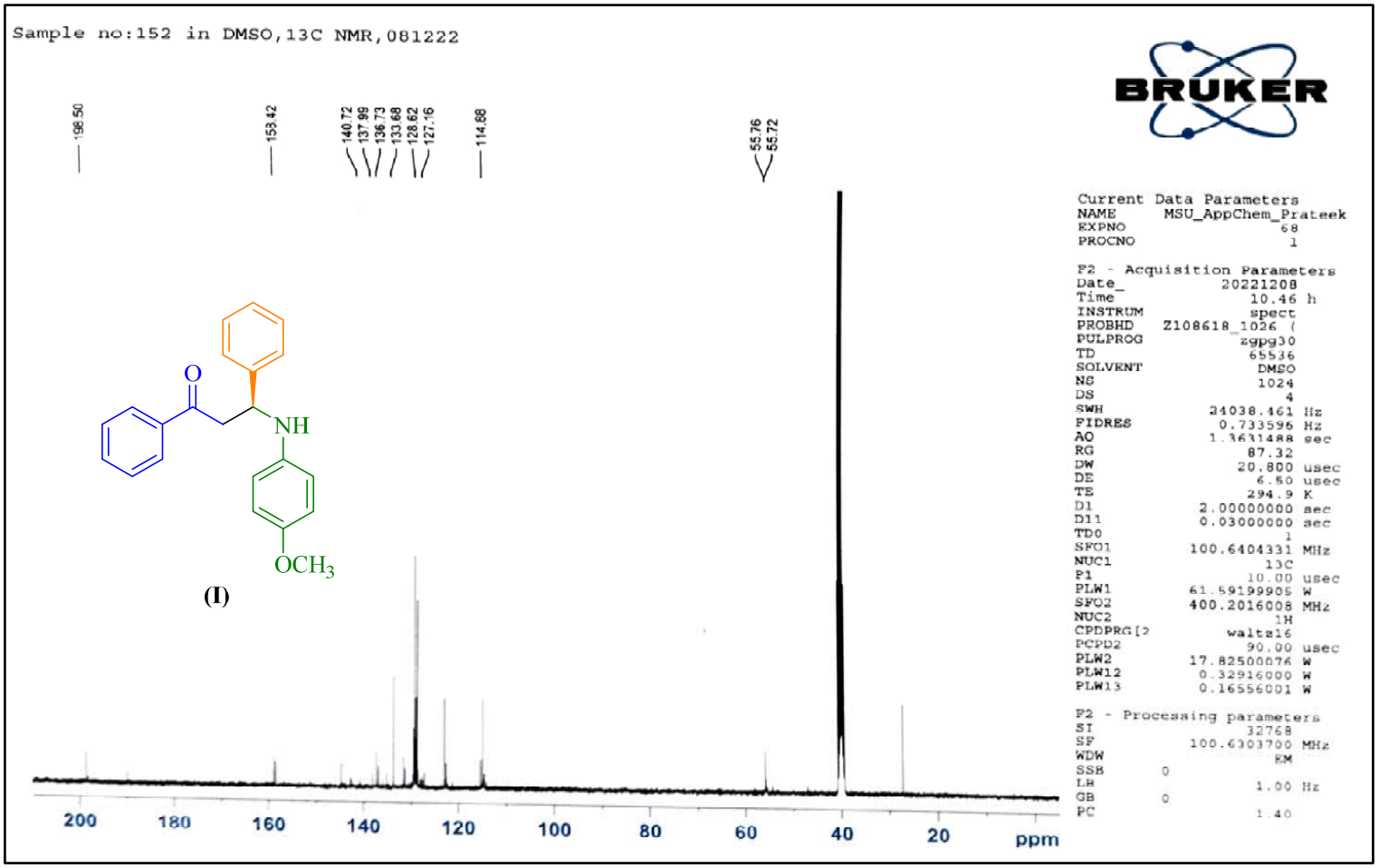

Fig. S51. ^{13}C NMR spectra of the product (I).

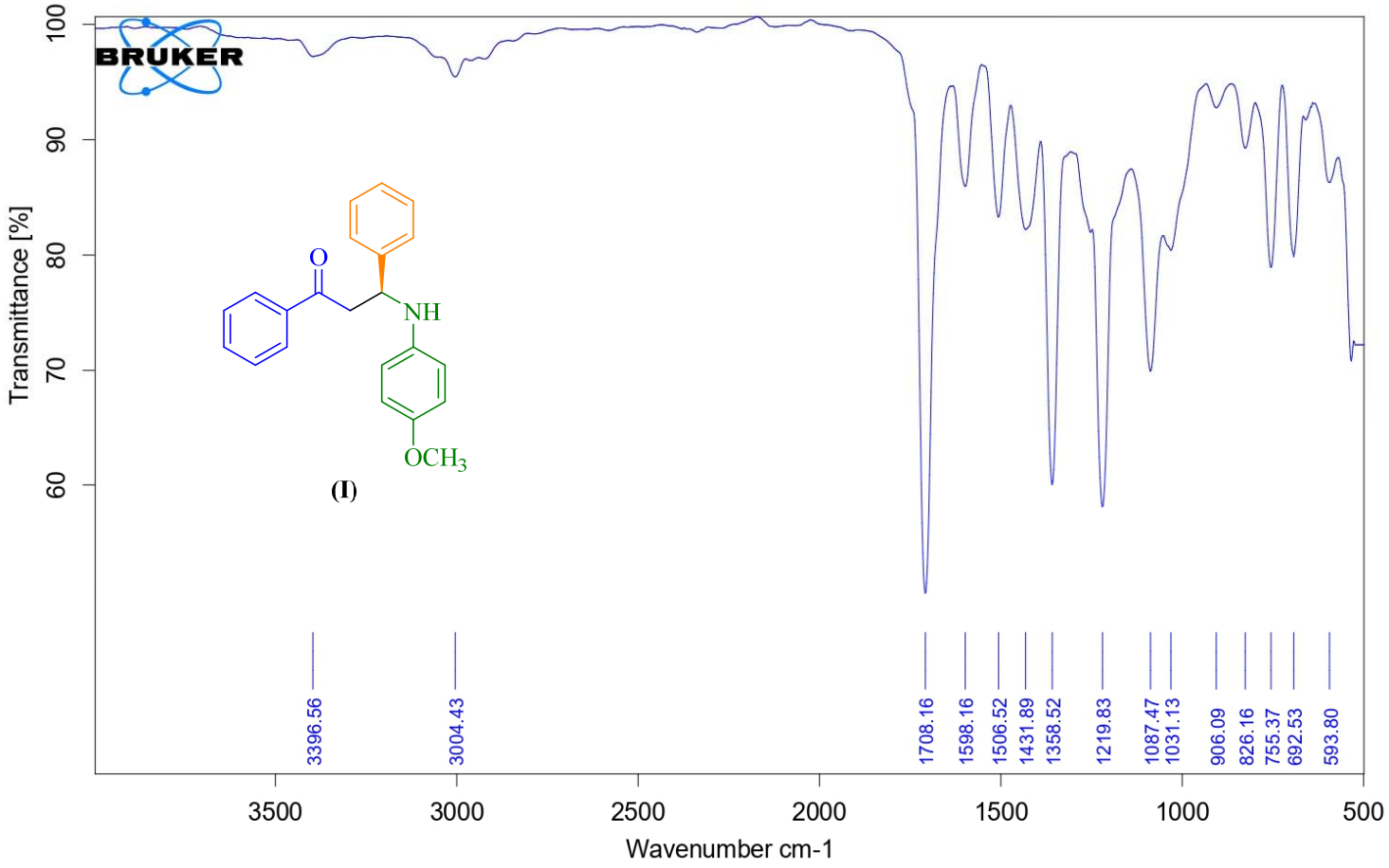

Fig. S52. FTIR spectra of the product (I).

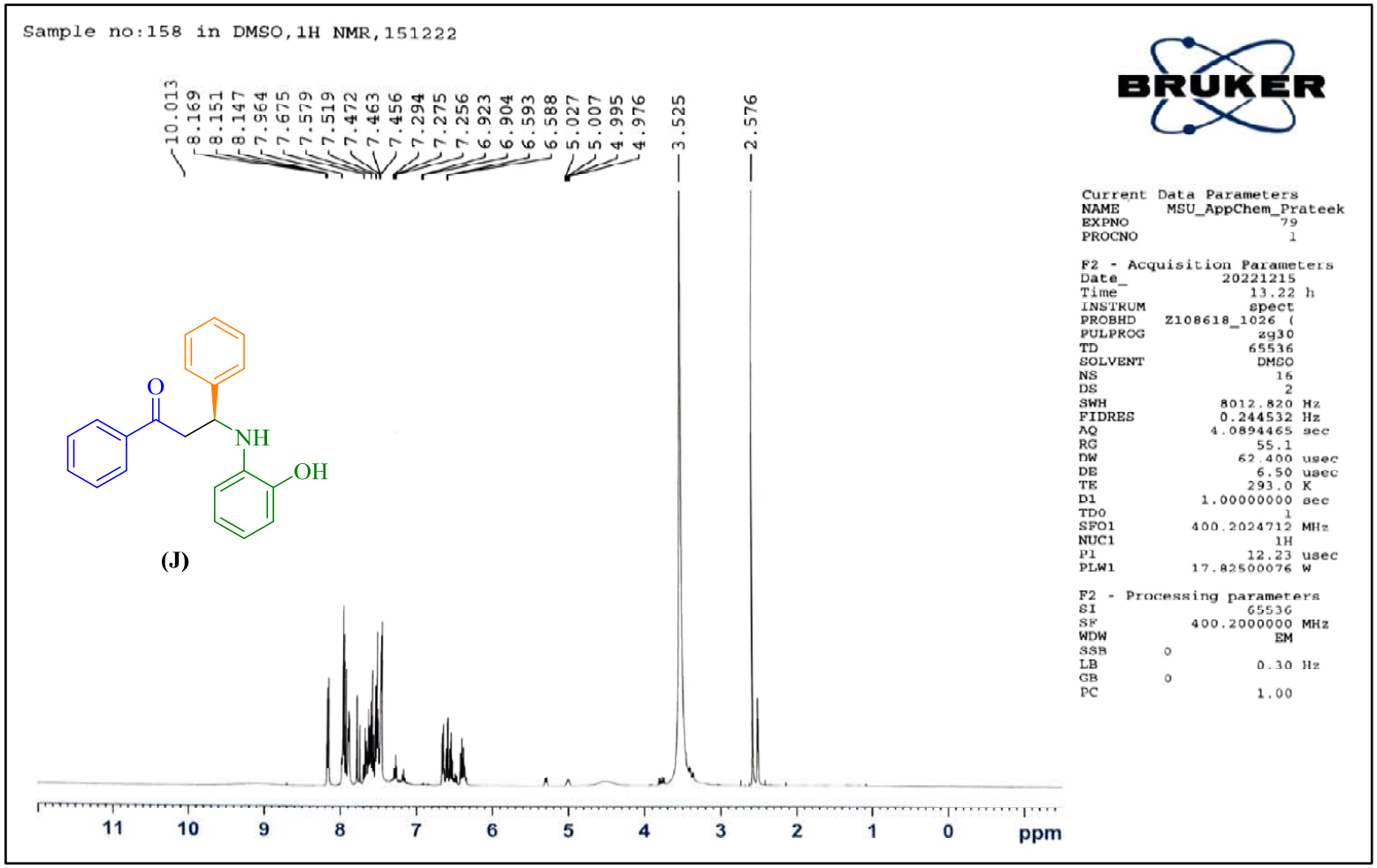

Fig. S53. ^{1}H NMR spectra of the product (J).

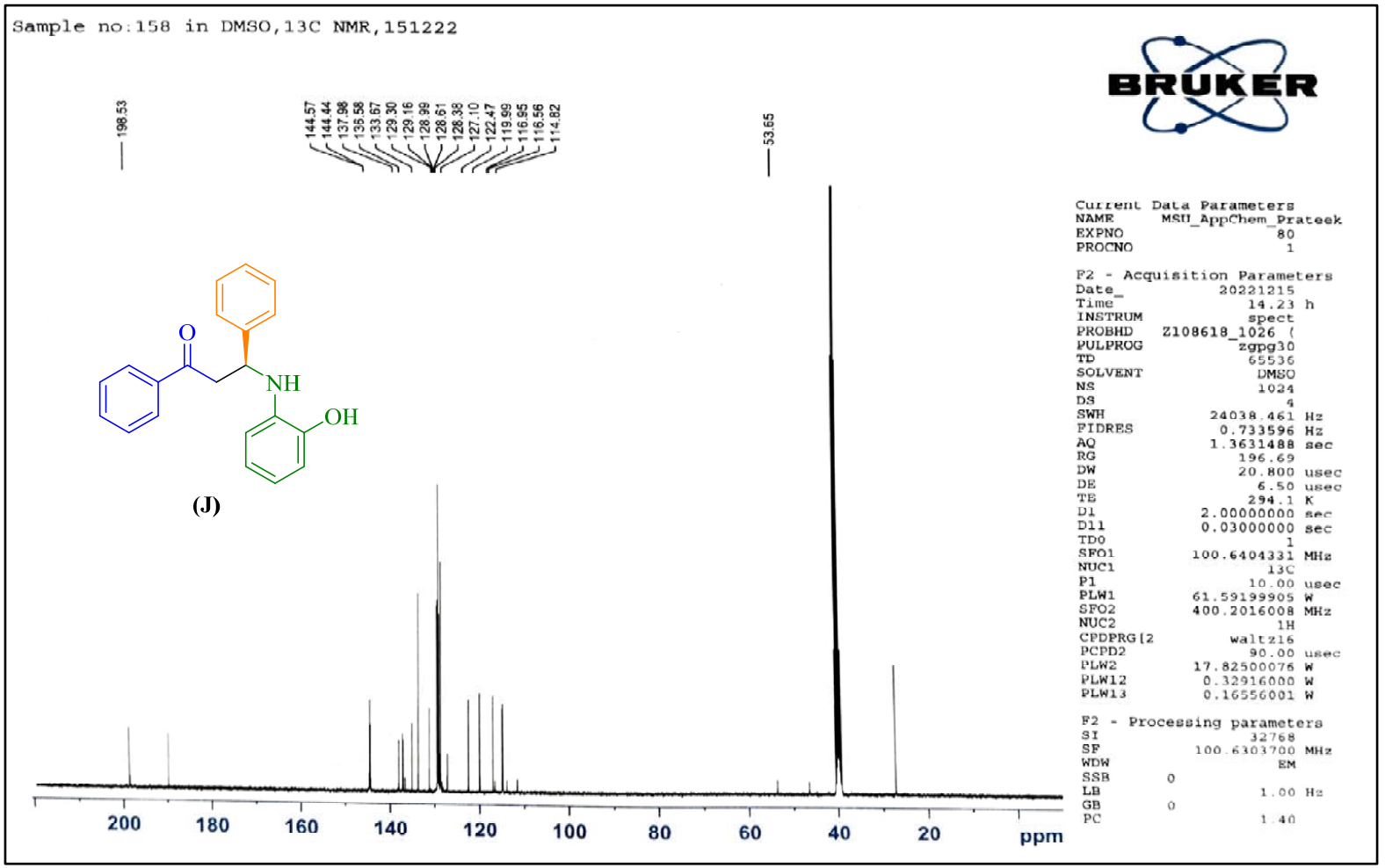

Fig. S54. ^{13}C NMR spectra of the product (J).

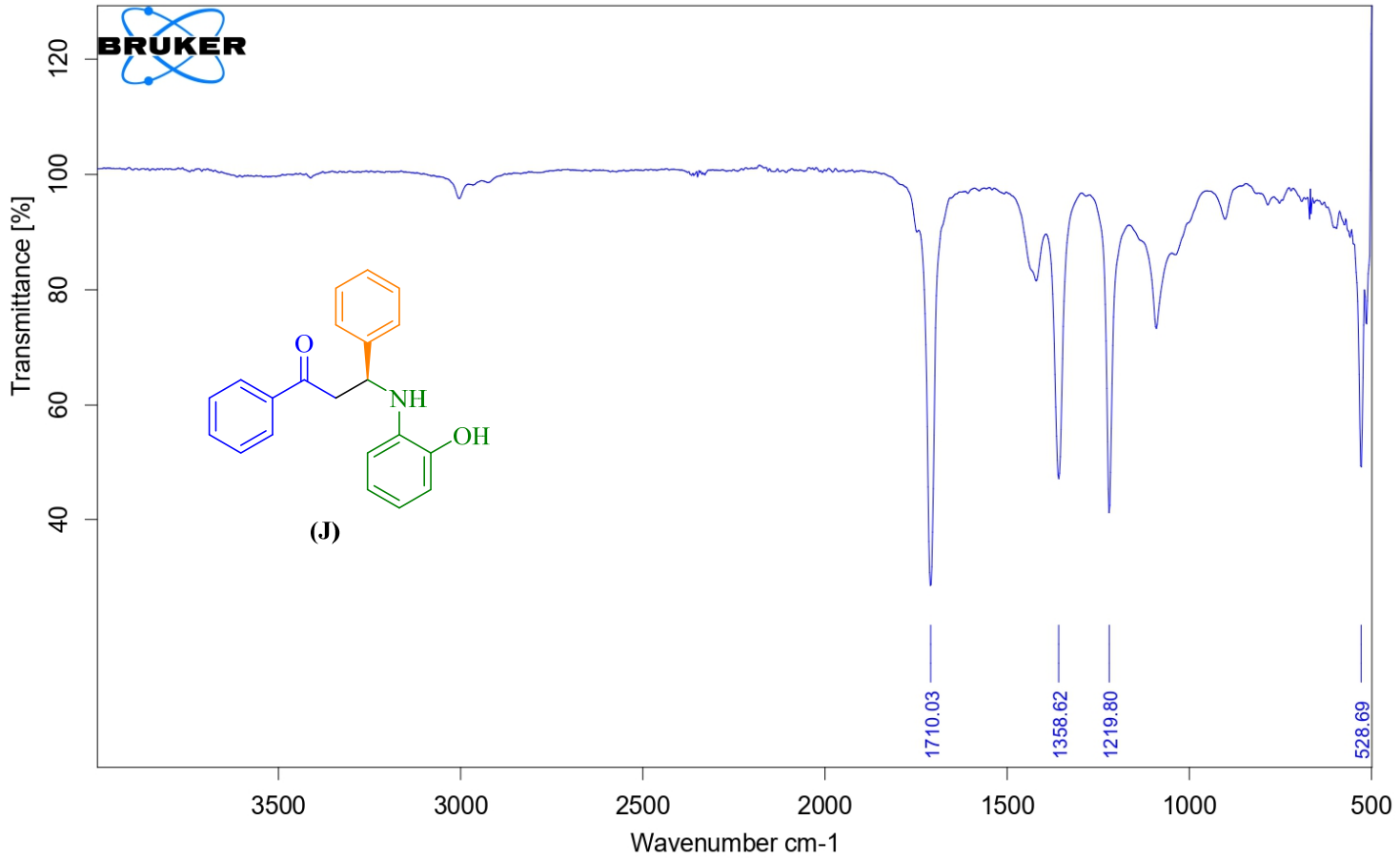

Fig. S55. FTIR spectra of the product (J).

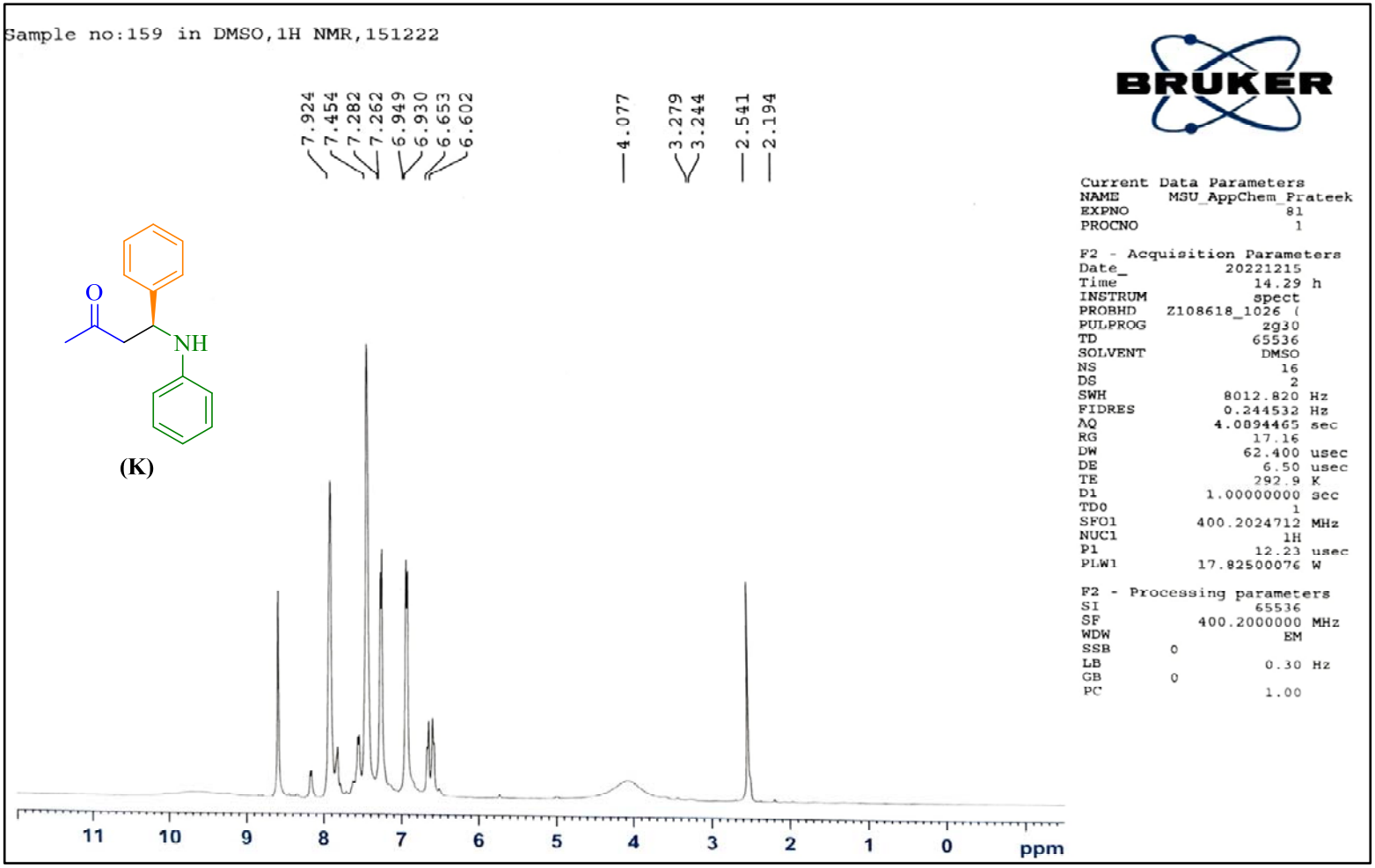

Fig. S56. ^{1}H NMR spectra of the product (K).

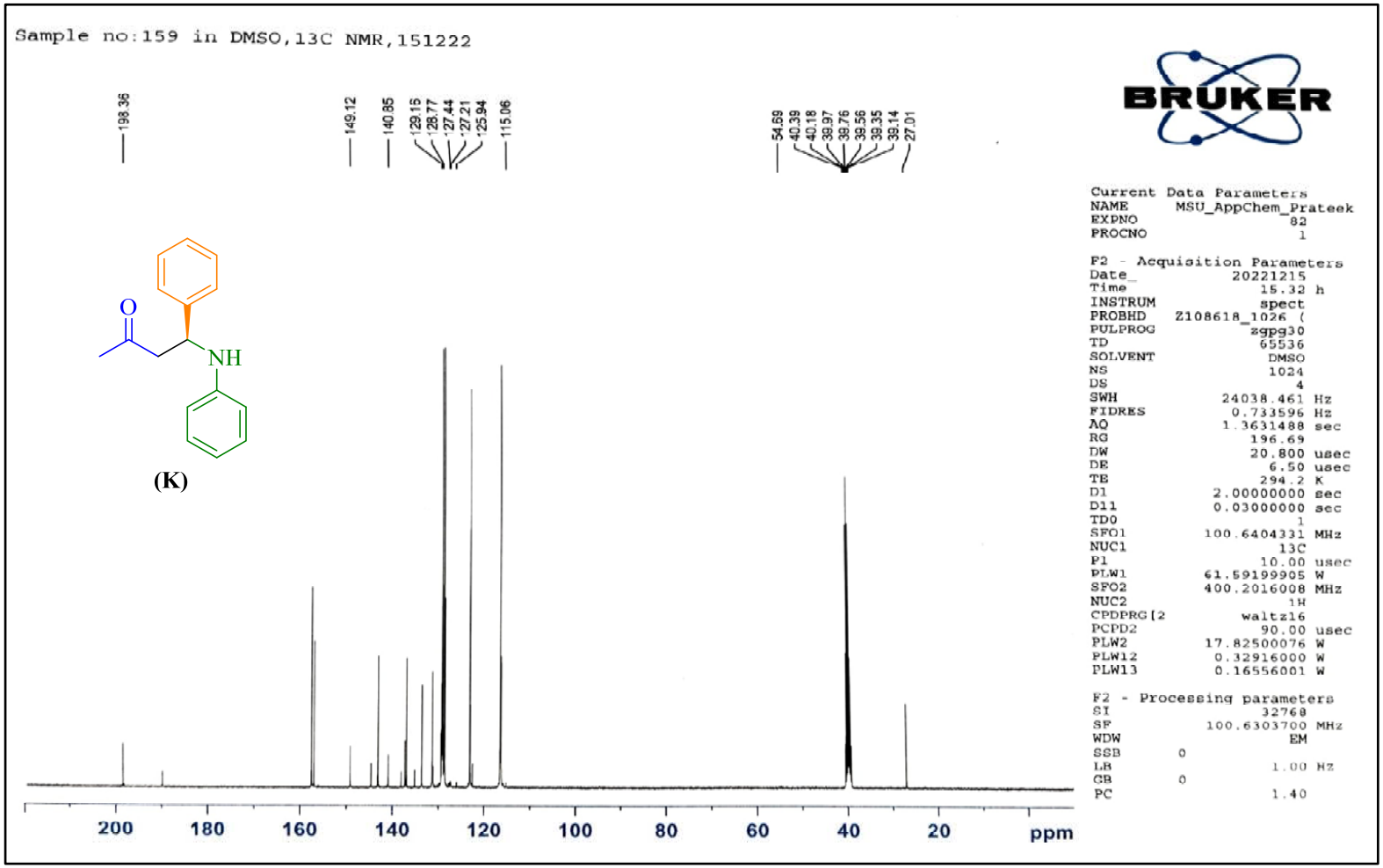

Fig. S57. ^{13}C NMR spectra of the product (K).

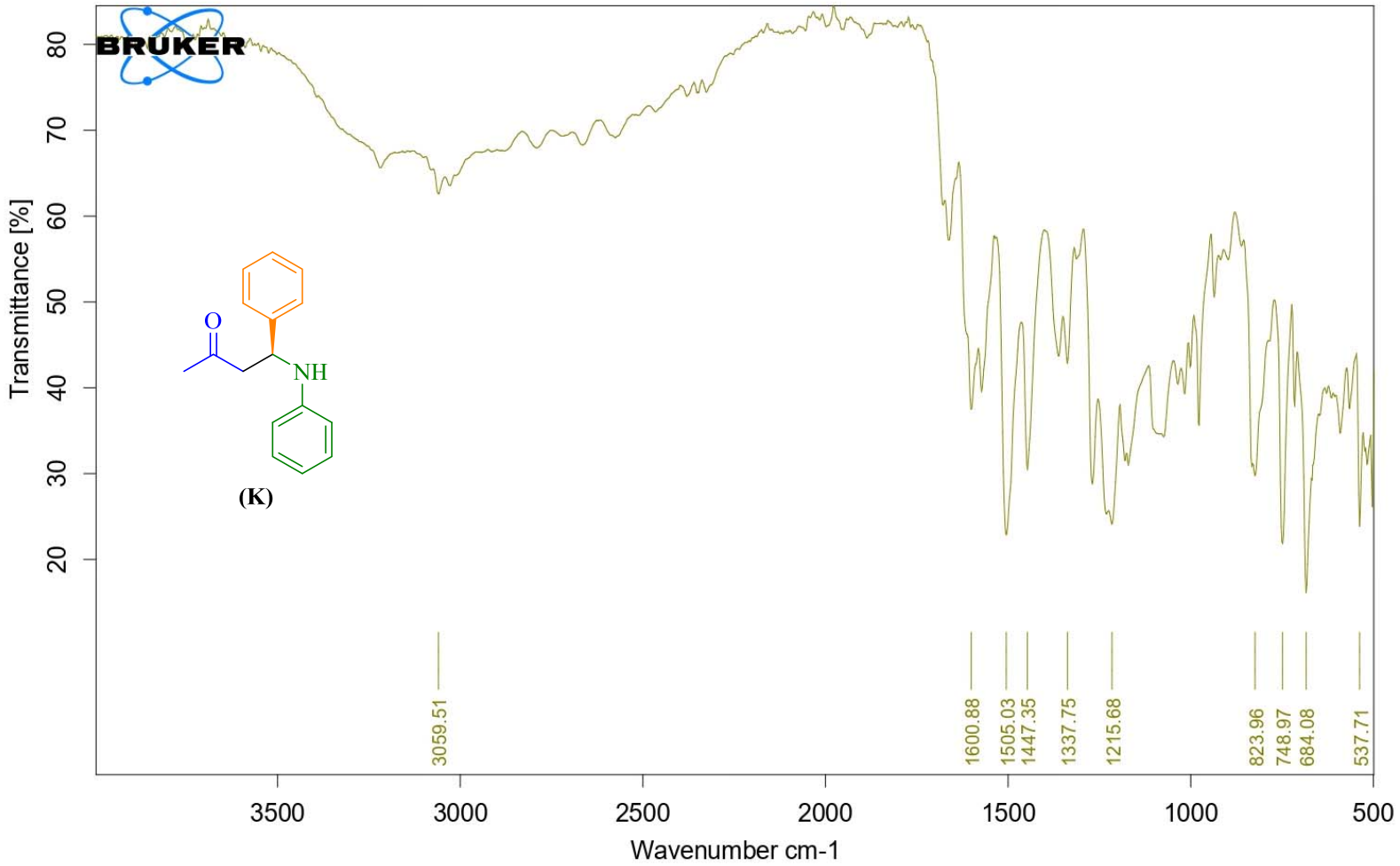

Fig. S58. FTIR spectra of the product (K).

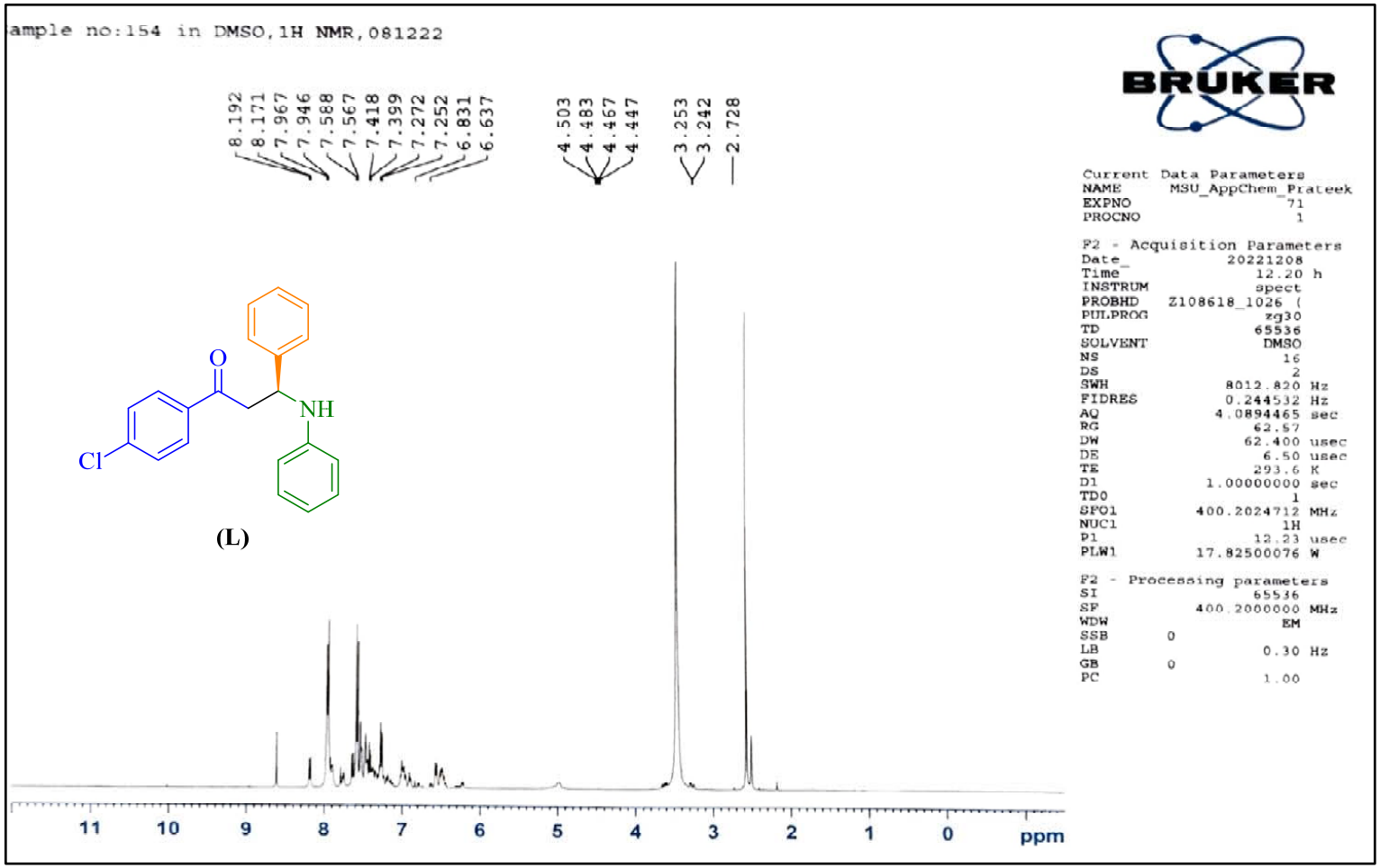

Fig. S59. ^{1}H NMR spectra of the product (L).

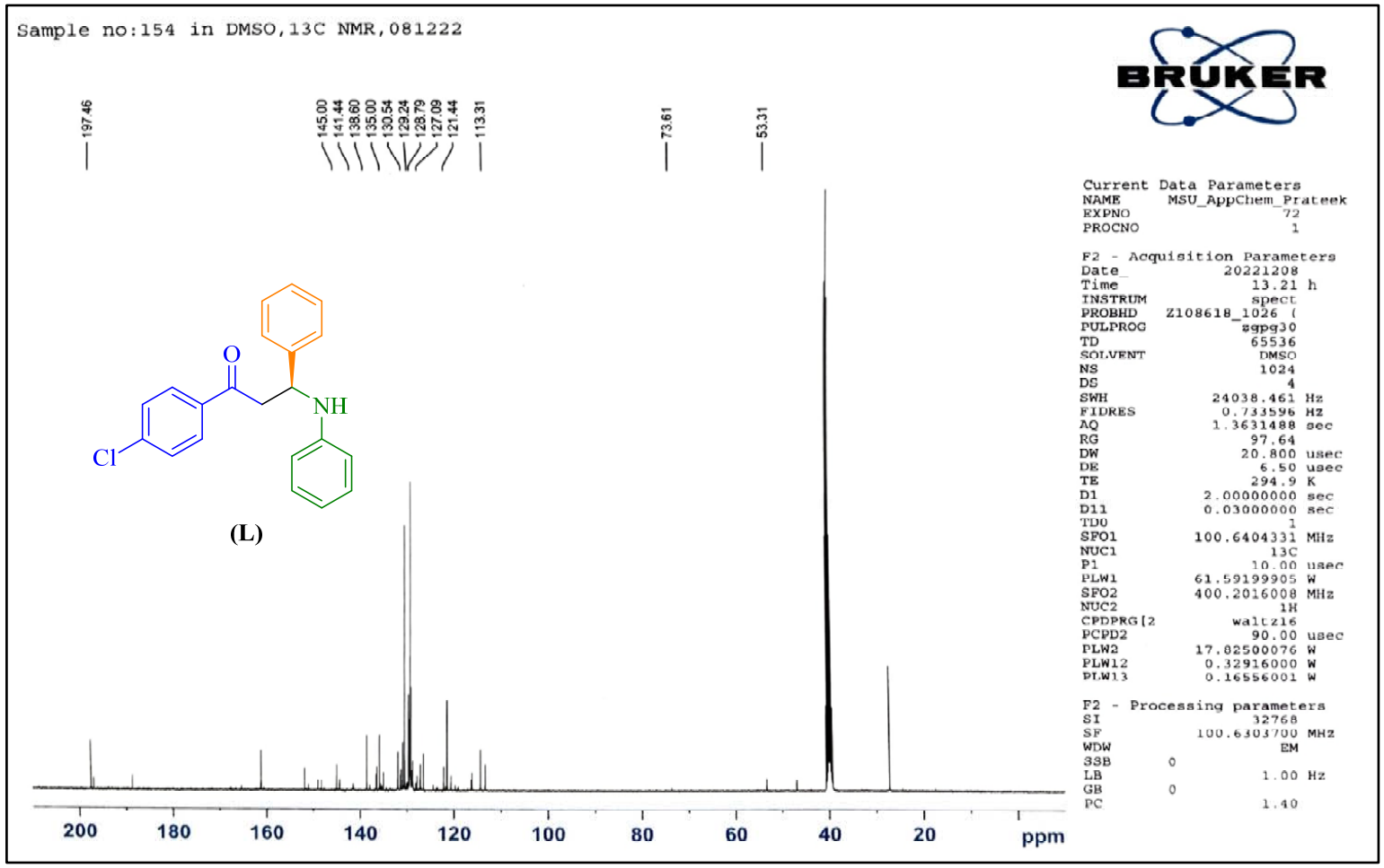

Fig. S60. ^{13}C NMR spectra of the product (L).

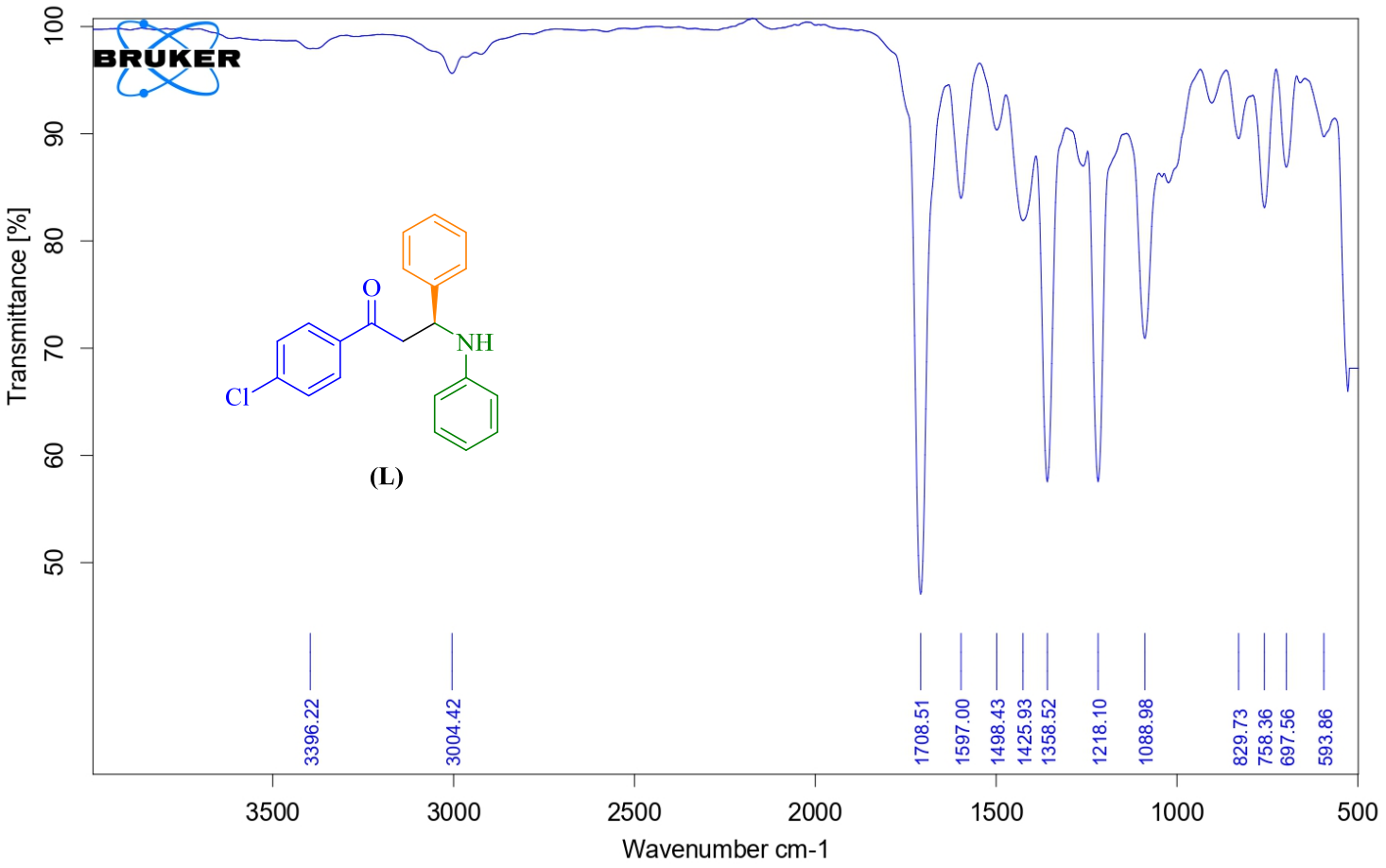

Fig. S61. FTIR spectra of the product (L).

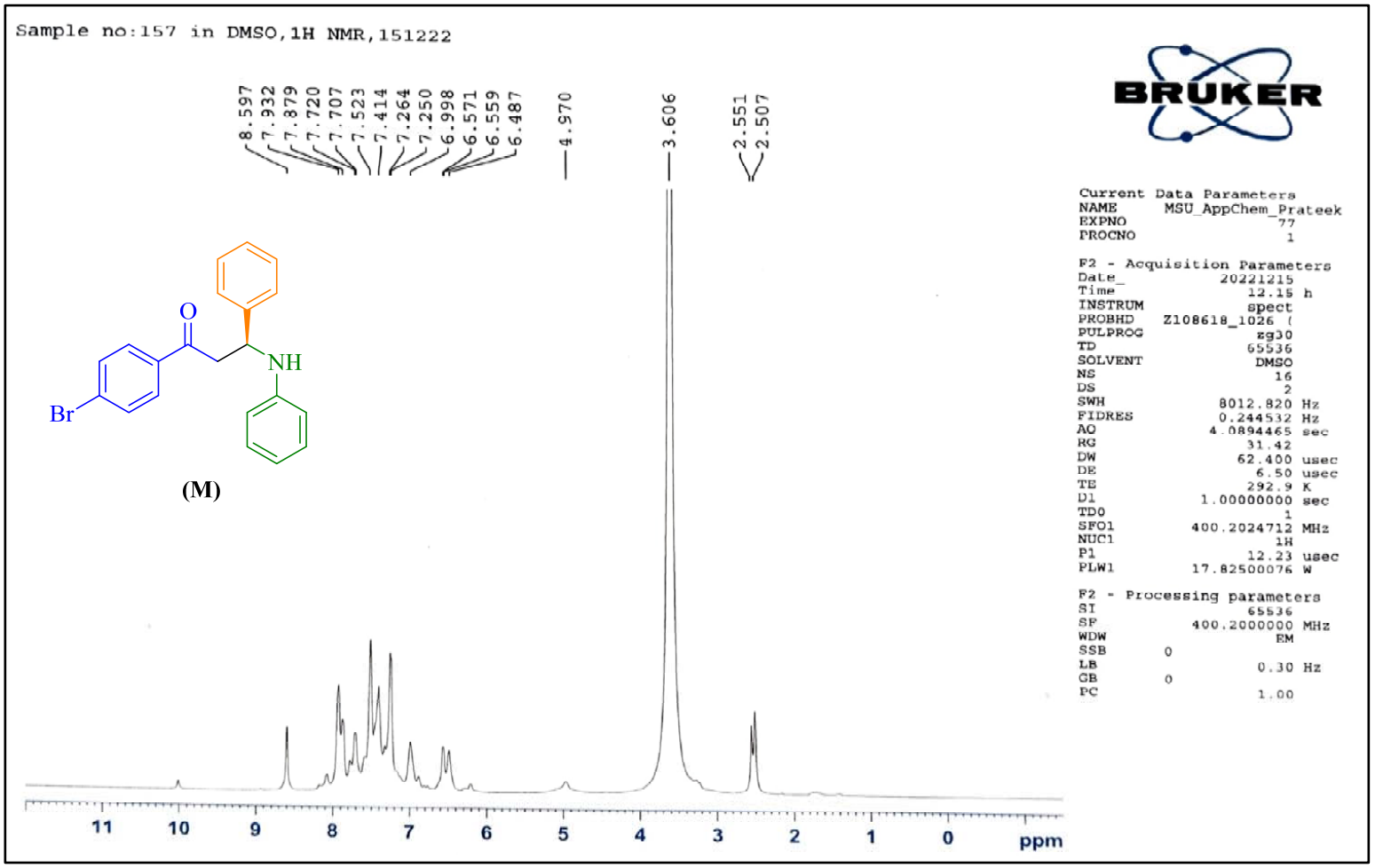

Fig. S62. ^{1}H NMR spectra of the product (M).

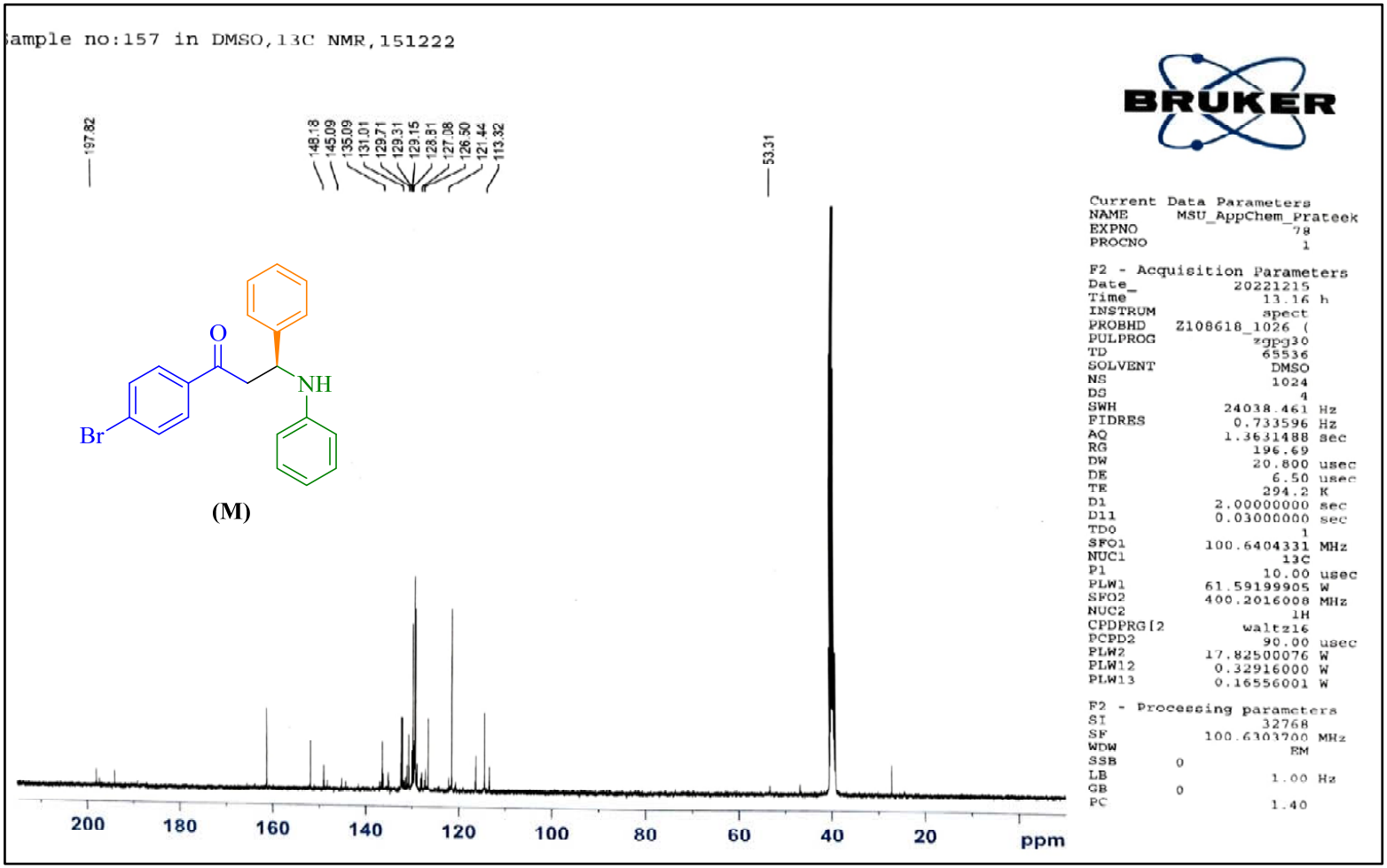

Fig. S63. ^{13}C NMR spectra of the product (M).

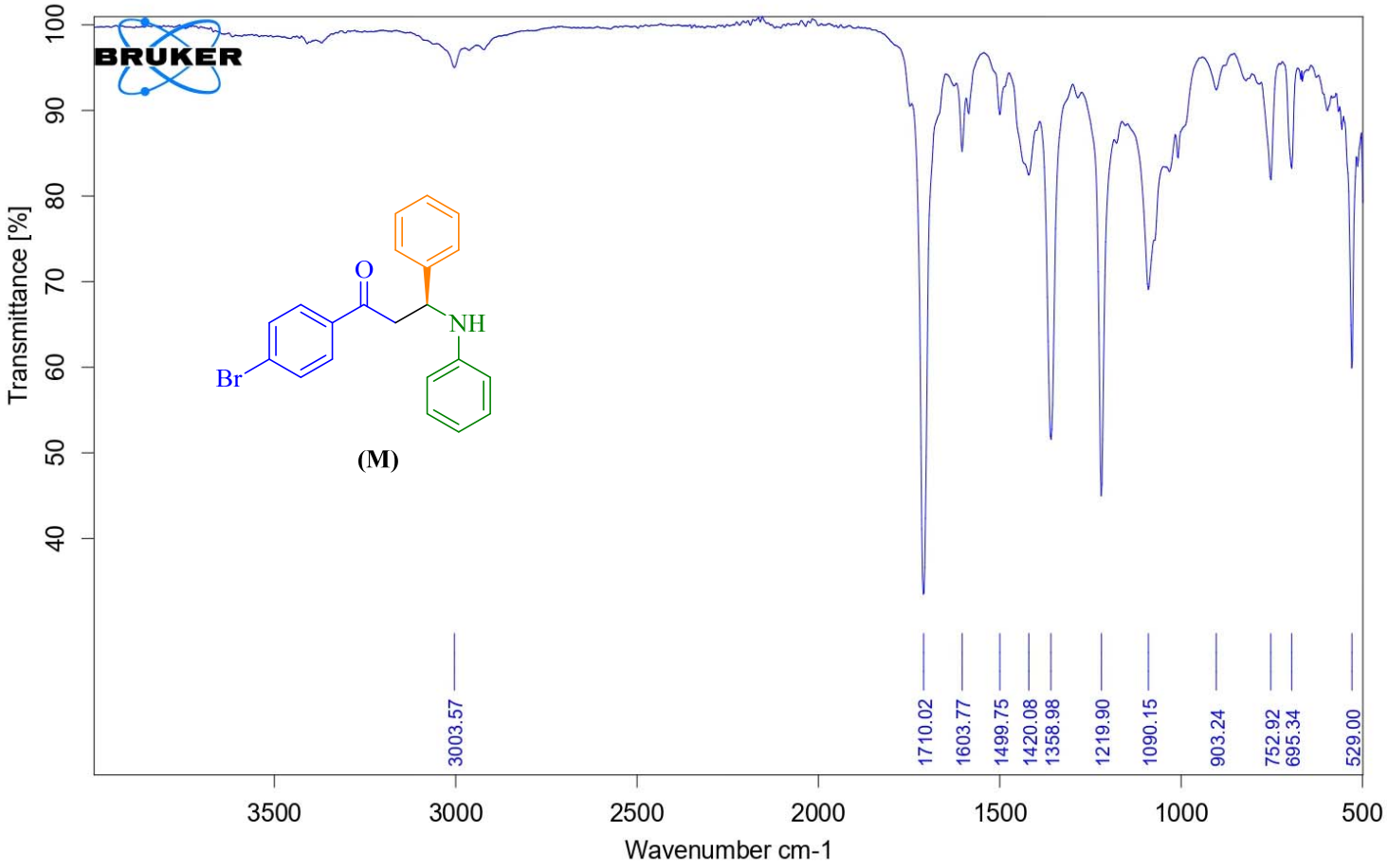

Fig. S64. FTIR spectra of the product (M).

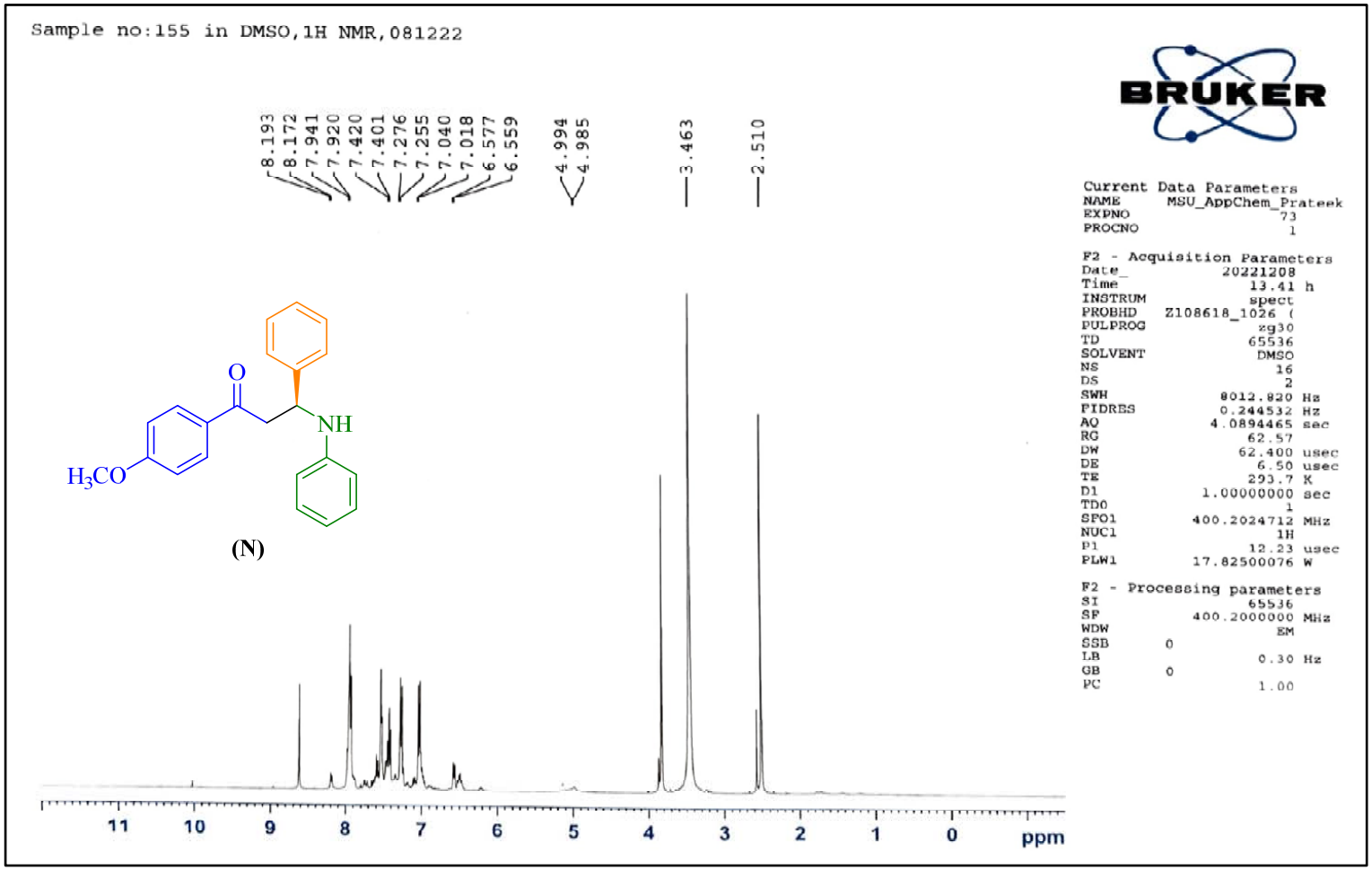

Fig. S65. ^{1}H NMR spectra of the product (N).

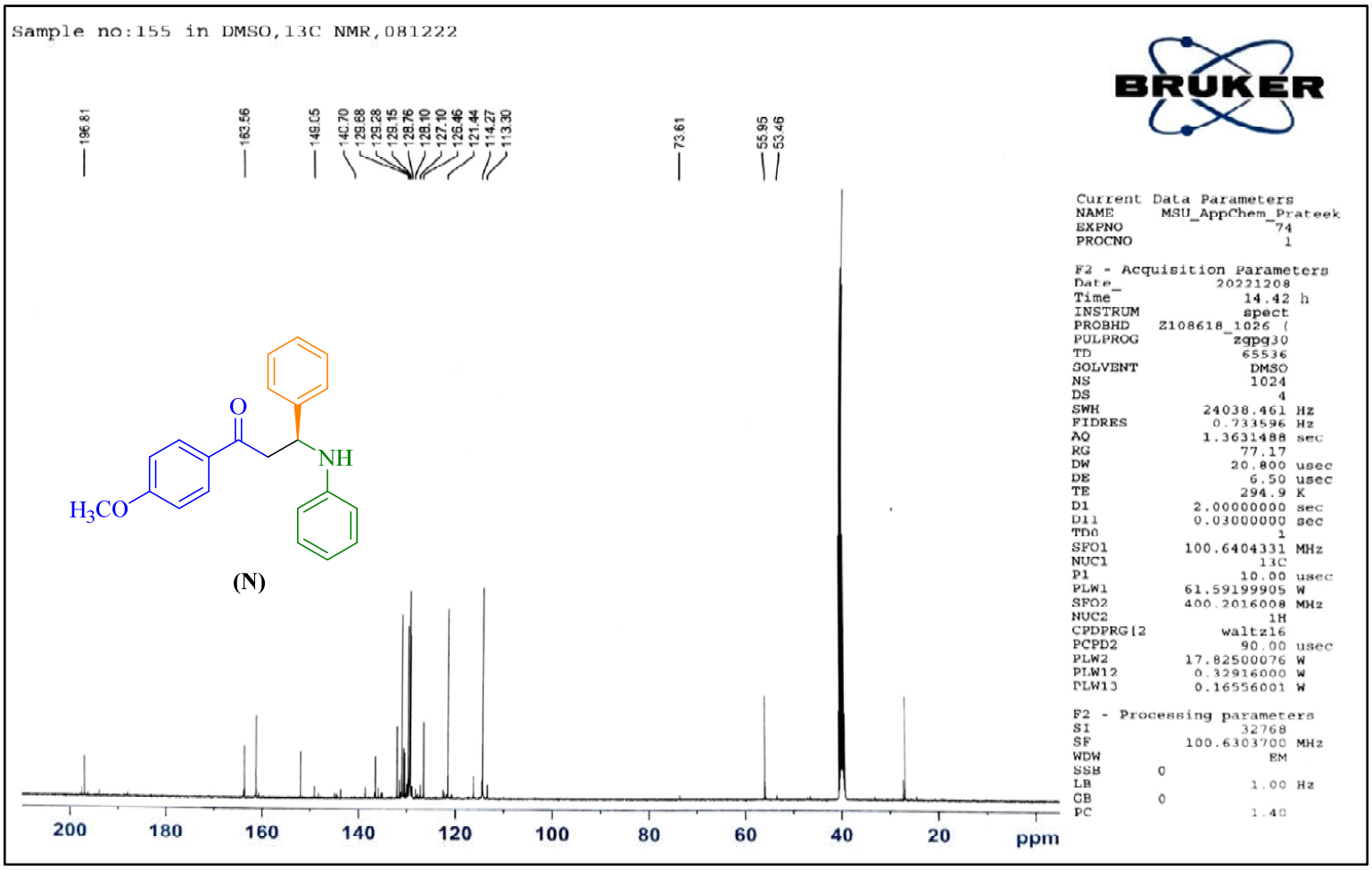

Fig. S66. ^{13}C NMR spectra of the product (N).

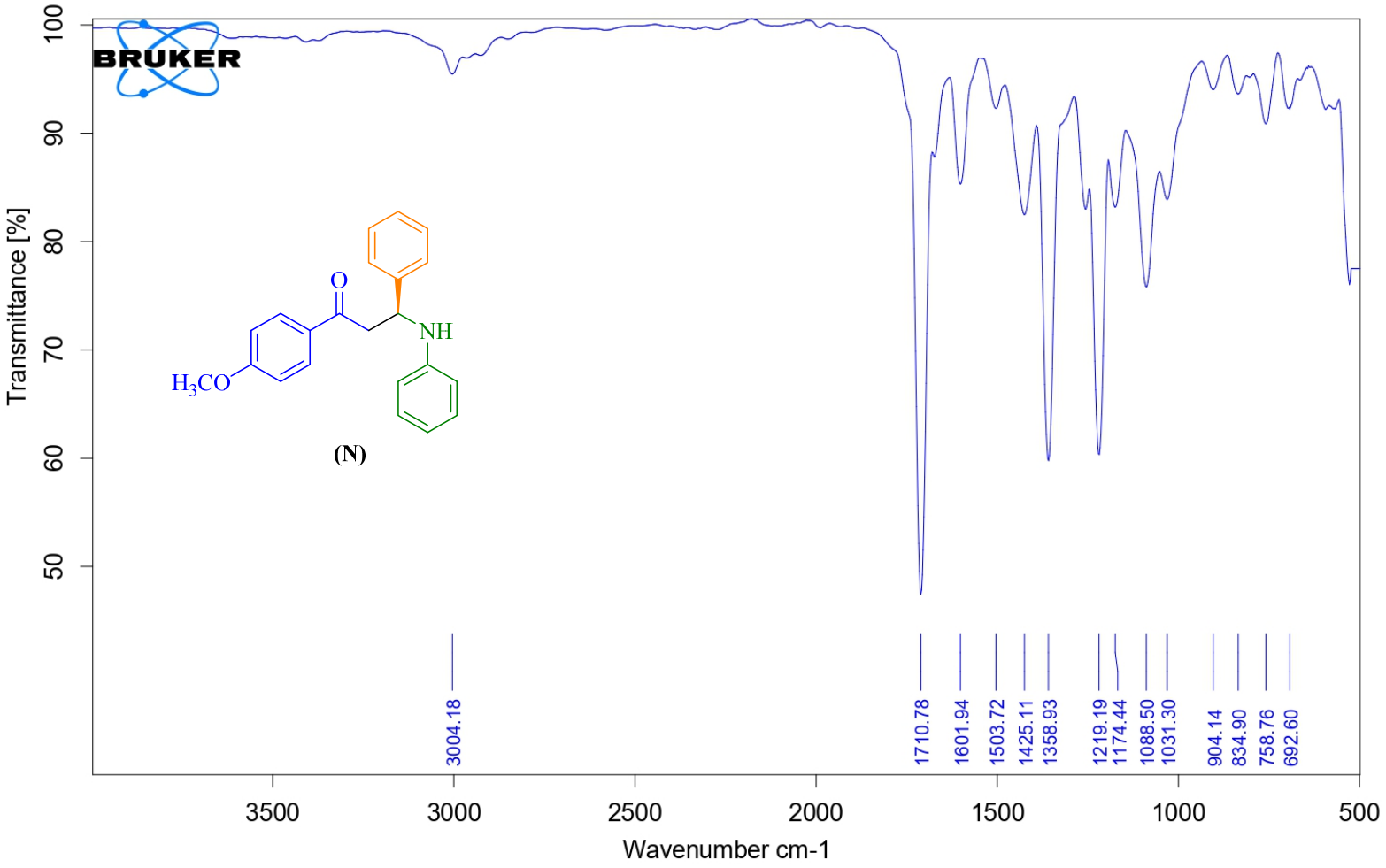

Fig. S67. FTIR spectra of the product (N).

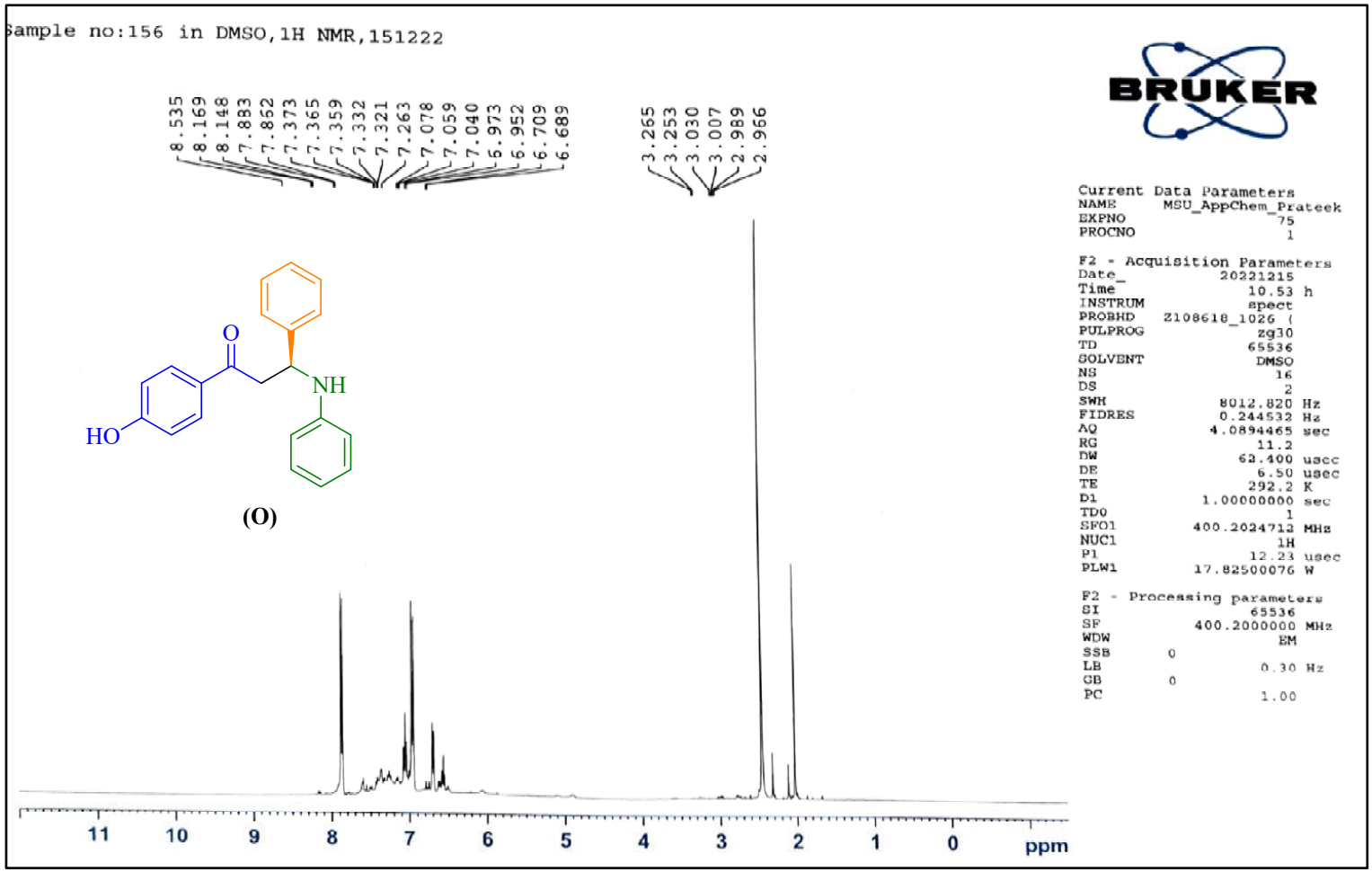

Fig. S68. ^{1}H NMR spectra of the product (O).

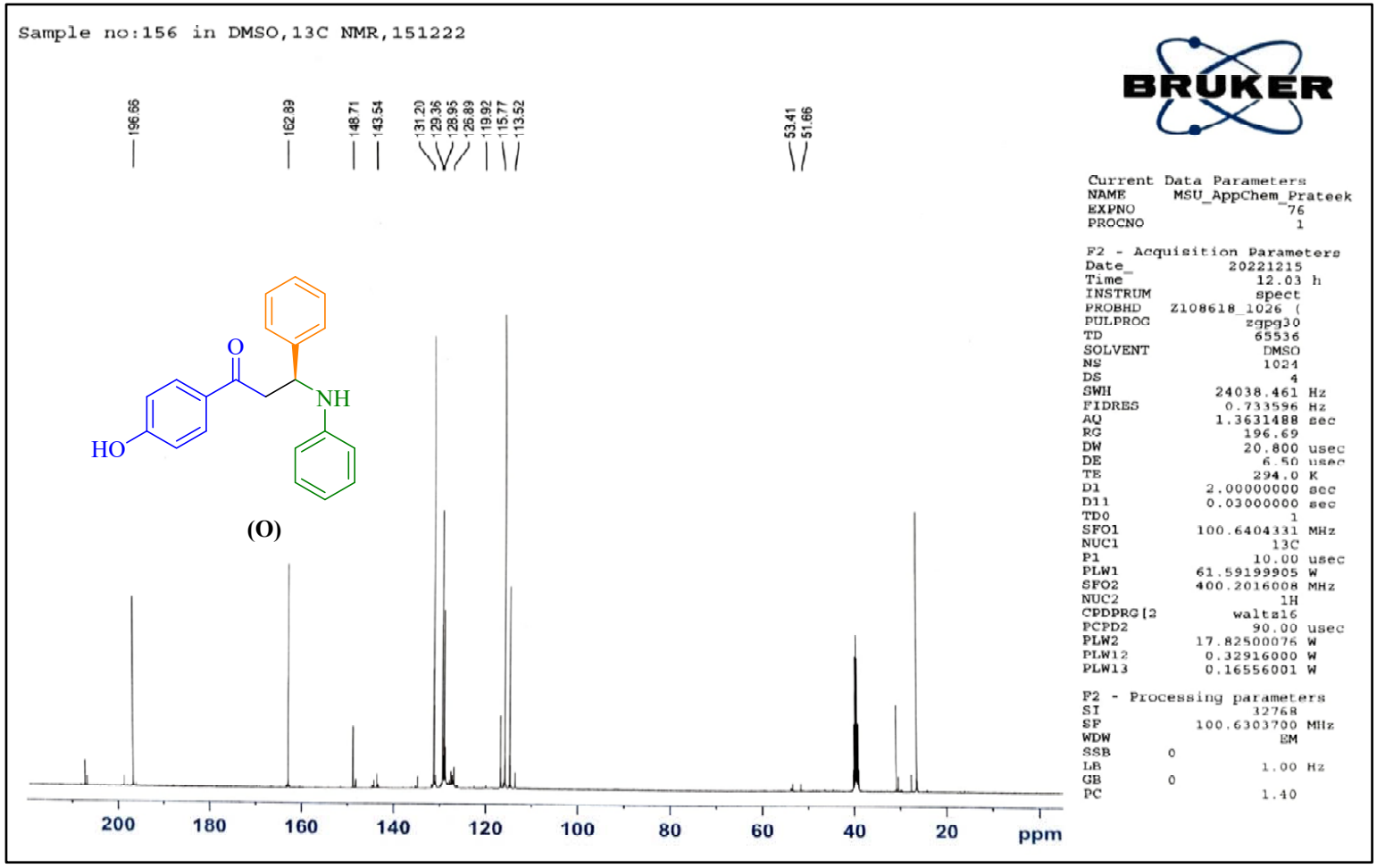

Fig. S69. ^{13}C NMR spectra of the product (O).

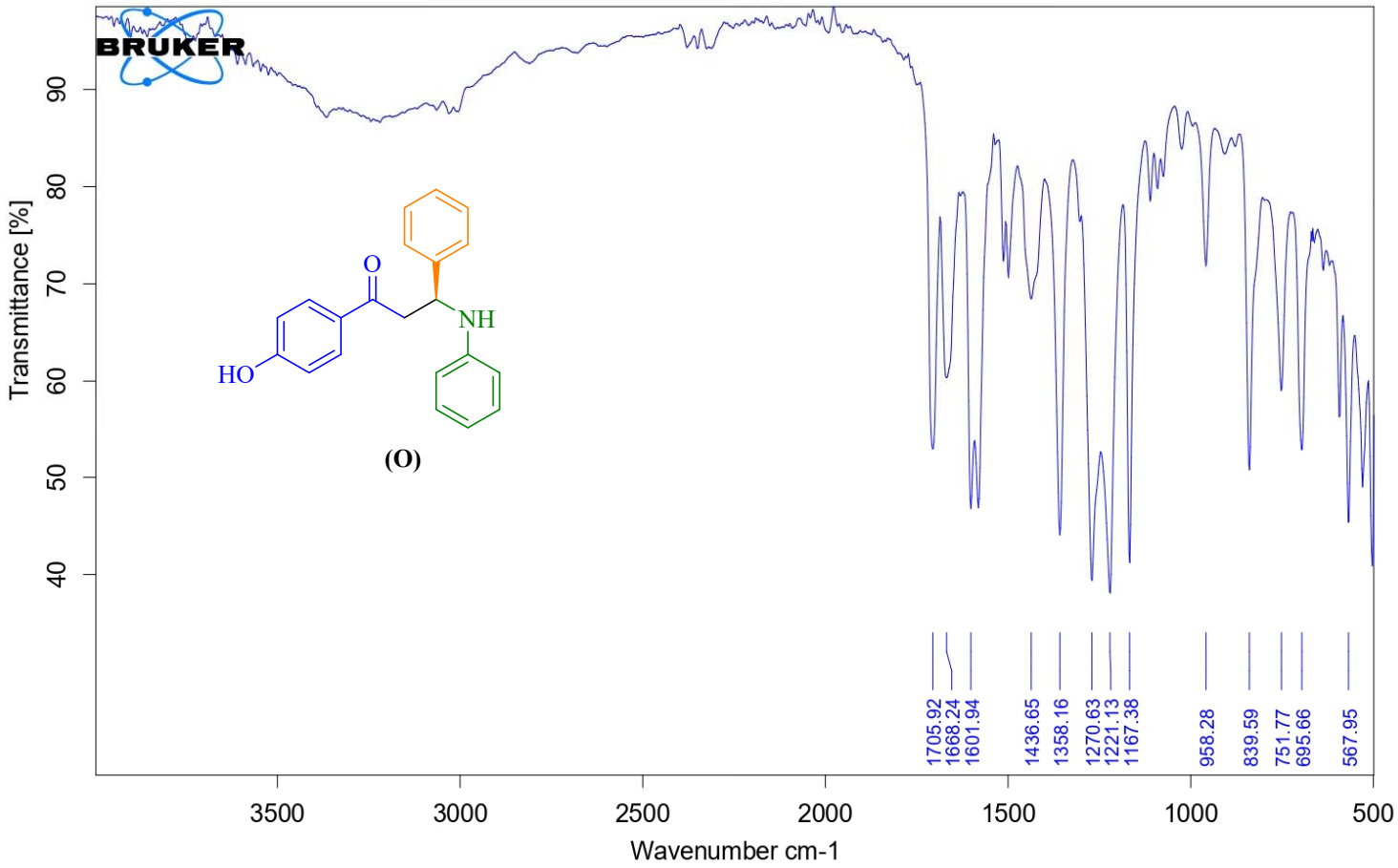

Fig. S70. FTIR spectra of the product (O).

7. Catalyst recyclability bar chart

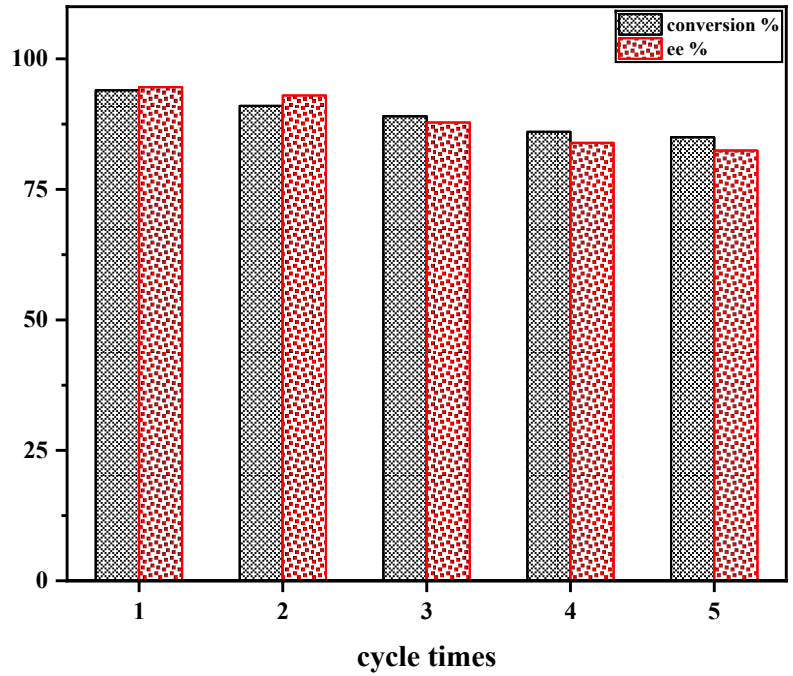

Fig. S71. Recyclability test of chiral Zn(II)-Salen@MWW catalyst over chiral β-aminoketones synthesis.

8. Characterization data of the catalyst after the 5th cycle

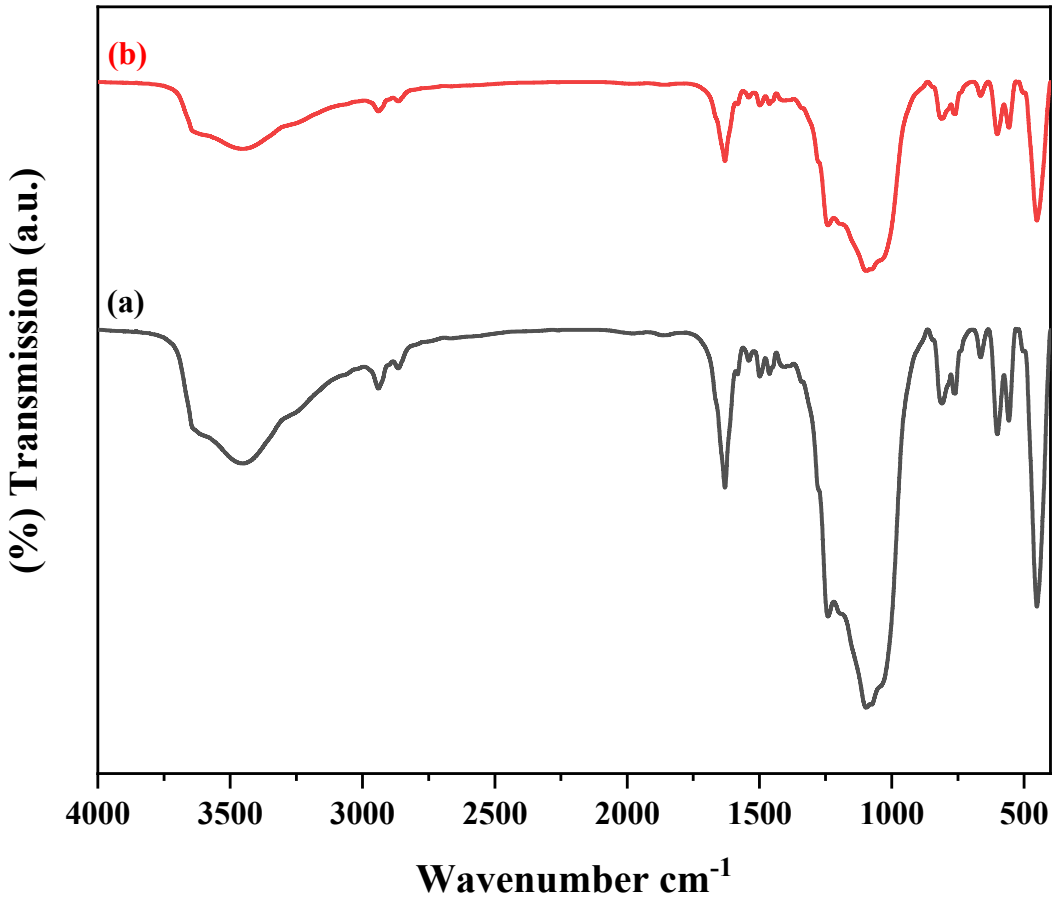

Fig. S72. FTIR spectra of (a) Fresh chiral Zn(II)-Salen@MWW catalyst and (b) Chiral Zn(II)-Salen@MWW catalyst after the 5th cycle

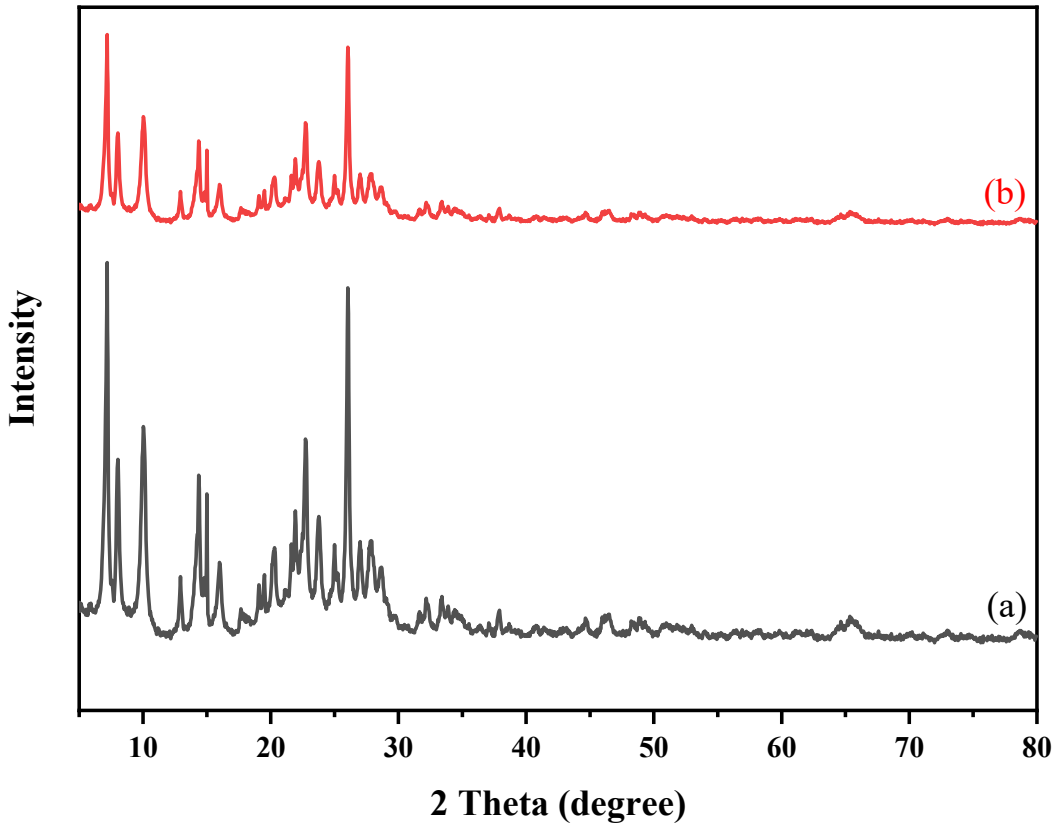

Fig. S73. XRD patterns of (a) Fresh chiral Zn(II)-Salen@MWW catalyst and (b) Chiral Zn(II)-Salen@MWW catalyst after the 5th cycle